



1 **Characteristics of PM_{2.5} mass concentrations and chemical species in urban and background**
2 **areas of China: emerging results from the CARE-China network**

3 Zirui Liu^{1*}, Wenkang Gao¹, Yangchun Yu¹, Bo Hu¹, Jinyuan Xin¹, Yang Sun¹, Lili Wang¹, Gehui
4 Wang³, Xinhui Bi⁴, Guohua Zhang⁴, Honghui Xu⁵, Zhiyuan Cong⁶, Jun He⁷, Jingsha Xu⁷, Yuesi
5 Wang^{1,2*}

6 ¹State Key Laboratory of Atmospheric Boundary Layer Physics and Atmospheric Chemistry, Institute of
7 Atmospheric Physics, Chinese Academy of Sciences, Beijing 100029, China

8 ²Center for Excellence in Regional Atmospheric Environment, Institute of Urban Environment, Chinese Academy
9 of Sciences, Xiamen 361021, China

10 ³State Key Laboratory of Loess and Quaternary Geology, Institute of Earth Environment, Chinese Academy of
11 Sciences, Xi'an 710075, China

12 ⁴State Key Laboratory of Organic Geochemistry, Guangzhou Institute of Geochemistry, Chinese Academy of
13 Sciences, Guangzhou 510640, China

14 ⁵Zhejiang Meteorology Science Institute, Hangzhou 310017, China

15 ⁶Key Laboratory of Tibetan Environment Changes and Land Surface Processes, Institute of Tibetan Plateau Research,
16 Chinese Academy of Sciences, Beijing 100101, China

17 ⁷International Doctoral Innovation Centre, The University of Nottingham Ningbo China, Ningbo 315100, China

18 *Corresponding author: Z.R Liu (Liuzirui@mail.iap.ac.cn); Y.S Wang (wys@mail.iap.ac.cn)

19

20 **Abstract:** The “Campaign on atmospheric Aerosol REsearch” network of China (CARE-China) is
21 a long-term project for the study of the spatiotemporal distributions of physical aerosol
22 characteristics as well as the chemical components and optical properties of aerosols over China.
23 This study presents the first long-term datasets from this project, including three years of
24 observations of online PM_{2.5} mass concentrations (2012-2014) and one year of observations of PM_{2.5}
25 compositions (2012-2013) from the CARE-China network. The average PM_{2.5} concentrations at 20
26 urban sites is 73.2 µg/m³ (16.8-126.9 µg/m³), which was three times higher than the average value
27 from the 12 background sites (11.2-46.5 µg/m³). The PM_{2.5} concentrations are generally higher in
28 east-central China than in the other parts of the country due to their relative large particulate matter
29 (PM) emissions and the unfavorable meteorological conditions for pollution dispersion. A distinct
30 seasonal variability of the PM_{2.5} is observed, with highs in the winter and lows during the summer
31 at urban sites. Inconsistent seasonal trends were observed at the background sites. Bimodal and
32 unimodal diurnal variation patterns were identified at both urban and background sites. The
33 chemical compositions of PM_{2.5} at six paired urban and background sites located within the most
34 polluted urban agglomerations and cleanest regions of China were analyzed. The major PM_{2.5}
35 constituents across all the urban sites are organic matter (OM, 26.0%), SO₄²⁻ (17.7%), mineral dust
36 (11.8%), NO₃⁻ (9.8%), NH₄⁺ (6.6%), elemental carbon (EC) (6.0%), Cl⁻ (1.2%) at 45% RH and
37 residual matter (20.7%). Similar chemical compositions of PM_{2.5} were observed at background sites
38 but were associated with higher fractions of OM (33.2%) and lower fractions of NO₃⁻ (8.6%) and
39 EC (4.1%). Significant variations of the chemical species were observed among the sites. At the
40 urban sites, the OM ranged from 12.6 µg/m³ (Lhasa) to 23.3 µg/m³ (Shenyang), the SO₄²⁻ ranged
41 from 0.8 µg/m³ (Lhasa) to 19.7 µg/m³ (Chongqing), the NO₃⁻ ranged from 0.5 µg/m³ (Lhasa) to 11.9
42 µg/m³ (Shanghai) and the EC ranged from 1.4 µg/m³ (Lhasa) to 7.1 µg/m³ (Guangzhou). The PM_{2.5}



43 chemical species at the background sites exhibited larger spatial heterogeneities than those at urban
44 sites, suggesting the different contributions from regional anthropogenic or natural emissions and
45 from the long-range transport to background areas. Notable seasonal variations of $PM_{2.5}$ polluted
46 days were observed, especially for the megacities in east-central China, resulting in frequent heavy
47 pollution episodes occurring during the winter. The evolution of the $PM_{2.5}$ chemical compositions
48 on polluted days was similar for the urban and nearby background sites, suggesting the significant
49 regional pollution characteristics of the most polluted areas of China. However, the chemical species
50 dominating the evolutions of the heavily polluted events were different in these areas, indicating
51 that unique mitigation measures should be developed for different regions of China. This analysis
52 reveals the spatial and seasonal variabilities of the urban and background aerosol concentrations on
53 a national scale and provides insights into their sources, processes, and lifetimes.

54

55

1. Introduction

56

Atmospheric fine particulate matter ($PM_{2.5}$) is a complex heterogeneous mixture, whose
57 physical size distribution and chemical composition change in time and space and are dependent on
58 the emission sources, atmospheric chemistry, and meteorological conditions (Seinfeld and Pandis,
59 2016). Atmospheric $PM_{2.5}$ has known important environmental impacts related to visibility
60 degradation and climate change. Because of their abilities to scatter and absorb solar radiation,
61 aerosols degrade visibility in both remote and urban locations and can have direct and indirect
62 effects on the climate (IPCC, 2013). Fine atmospheric particles are also a health concern and have
63 been linked to respiratory and cardiovascular diseases (Sun et al., 2010; Viana et al., 2008; Zhang
64 et al., 2014a). The magnitudes of the effects of $PM_{2.5}$ on all these systems depend on their sizes and
65 chemical compositions. Highly reflective aerosols, such as sulfates and nitrates, result in direct
66 cooling effects, while aerosols with low single-scattering albedos absorb solar radiation and include
67 light-absorbing carbon, humic-like substances, and some components of mineral soils (Hoffer et al.,
68 2006). The health impacts of these particles may also differ with different aerosol compositions
69 (Zimmermann, 2015); the adverse health effects specifically associated with organic aerosols have
70 been reported by Mauderly and Chow (2008). Therefore, the uncertainties surrounding the roles of
71 aerosols in climate, visibility, and health studies can be significant because chemical composition
72 data may not be available for large spatial and temporal ranges.

73

Reducing the uncertainties associated with aerosol effects requires observations of aerosol
74 mass concentrations and chemical speciation from long-term spatially extensive ground-based
75 networks. Continental sampling using ground-based networks has been conducted in North America
76 (Hand et al., 2012) and Europe (Putaud et al., 2010) since the 1980s, such as via the U.S. EPA's
77 Chemical Speciation Network (CSN), the Interagency Monitoring of Protected Visual Environments
78 (IMPROVE) network, the Clean Air Status and Trends Network (CASTNET) and the National
79 Atmospheric Deposition Program (NADP). Previous studies suggest the spatial and temporal
80 patterns of $PM_{2.5}$ mass concentrations and chemical species can vary significantly depending on
81 species and location. For example, Malm et al. (2004) reported the 2001 monthly mean speciated
82 aerosol concentrations from the IMPROVE monitors across the United States and demonstrated that
83 ammonium sulfate concentrations were highest in the eastern United States and dominated the fine
84 particle masses in the summer. Clearly decreasing gradients of the SO_4^{2-} and NO_3^- contributions to



85 PM_{10} were observed in Europe when moving from rural to urban to kerbside sites (Putaud et al.,
86 2010). Although large disparities of $PM_{2.5}$ pollution levels exist between those megacities in
87 developing and developed countries, the $PM_{2.5}$ annual mass concentrations in the former are
88 approximately 10 times greater than those of the latter (Cheng et al., 2016); however, ground-based
89 networks that consistently measures $PM_{2.5}$ mass concentrations and chemical compositions remain
90 rare in the densely populated regions of developing countries.

91 China is the world's most populous country and has one of the fastest-growing economies. Fast
92 urbanization and industrialization can cause considerable increases in energy consumption. China's
93 energy consumption increased 120% from 2000 to 2010. Coal accounted for most of the primary
94 energy consumption (up to 70%) (Department of Energy Statistics, National Bureau of Statistics of
95 China, 2001; 2011). Meanwhile, the emissions of high concentrations of numerous air pollutants
96 cause severe air pollution and haze episodes. For example, a heavy air pollution episode occurred
97 in northeastern China in January of 2013, wherein the maximum hourly averaged $PM_{2.5}$ exceeded
98 $600 \mu\text{g m}^{-3}$ in Beijing (Wang et al., 2014). This event led to considerable public concern. However,
99 ground-based networks that consistently measure $PM_{2.5}$ mass concentrations and chemical
100 compositions in China are limited. Although there were some investigations of the various aerosol
101 chemical compositions in China (He et al., 2001; Huang et al., 2013; Li et al., 2012; Liu et al., 2015;
102 Pan et al., 2013; Tao et al., 2014; Wang et al., 2013; Yang et al., 2011; Zhao et al., 2013a; Zhou et
103 al., 2012), earlier studies were limited in their temporal and spatial scopes, with very few having
104 data exceeding one year while covering various urban and remote regions of the country (Zhang et
105 al., 2012; Wang et al., 2015). Indeed, before 2013, the Chinese national monitoring network did not
106 report measurements of $PM_{2.5}$ or its chemical composition, and thus, ground-based networks for
107 atmospheric fine particulate matter measurements at regional and continental scales are needed as
108 these networks are essential for the development and implementation of effective air pollution
109 control strategies and are also useful for the evaluation of regional and global models and satellite
110 retrievals.

111 To meet these sampling needs, the "Campaign on atmospheric Aerosol REsearch" network of
112 China (CARE-China) was established in late 2011 for the study of the spatiotemporal distributions
113 of the physical and chemical characteristics and optical properties of aerosols (Xin et al., 2015).
114 This study presents the first long-term dataset to include three years of observations of online $PM_{2.5}$
115 mass concentrations (2012-2014) and one year of observations of $PM_{2.5}$ compositions (2012-2013)
116 from the CARE-China network. The purpose of this work is to (1) assess the $PM_{2.5}$ mass
117 concentration levels, including the seasonal and diurnal variation characteristics at the urban, rural
118 and regional background sites; to (2) obtain the seasonal variations of the $PM_{2.5}$ chemical
119 compositions at paired urban/background sites in the most polluted regions and clean areas; and to
120 (3) identify the occurrences and chemical signatures of haze events via an analysis of the temporal
121 evolutions and chemical compositions of $PM_{2.5}$ on polluted days. These observations and analyses
122 provide general pictures of atmospheric fine particulate matter in China and can also be used to
123 validate model results and implement effective air pollution control strategies.

124 **2 Materials and methods**

125 **2.1 An introduction to the $PM_{2.5}$ monitoring sites**

126 The $PM_{2.5}$ data from 36 ground observation sites used in this study were obtained from the



127 CARE-China network (Campaign on the atmospheric Aerosol REsearch network of China), which
128 was supported by the Chinese Academy of Sciences (CAS) Strategic Priority Research Program
129 grants (Category A). Xin et al. (2015) provided an overview of the CARE-China network, the cost-
130 effective sampling methods employed and the post-sampling instrumental methods of analysis. Four
131 more ground observation sites (Shijiazhuang, Tianjin, Ji'nan and Lin'an) from the "Forming
132 Mechanism and Control Strategies of Haze in China" group (Wang et al., 2014) were also included
133 in this study to better depict the spatial distributions and temporal variations of the PM_{2.5} in eastern
134 China. A comprehensive 3-year observational network campaign from 2012 to 2014 was carried out
135 at these 40 ground observation sites. Figure 1 and Table 1, respectively, show the geographic
136 distribution and details of the network stations, which include 20 urban sites, 12 background sites
137 and 8 rural/suburban sites. The urban sites, such as those at Beijing, Shanghai and Guangzhou, are
138 locations surrounded by typical residential areas and commercial districts. The background sites are
139 located in natural reserve areas or scenic spots, which are far away from anthropogenic emissions
140 and are less influenced by human activities. Rural/suburban sites are situated in rural and suburban
141 areas, which may be affected by agricultural activities, vehicle emissions and some light industrial
142 activities. These sites are located in different parts of China and can provide an integrated insight
143 into the characteristic of PM_{2.5} over China.

144 **2.2 Online instruments and data sets**

145 A tapered element oscillating microbalance (TEOM) was used for the PM_{2.5} measurements at
146 thirty-four sites within the network (Table S1). This system was designated by the US
147 Environmental Protection Agency (USEPA) as having a monitoring compliance equivalent to the
148 National Ambient Air Quality standard for particulate matter (Patashnick and Rupprecht 1991). The
149 measurement ranges of the TEOMs were 0-5 g/m³, with a 0.1 µg/m³ resolution and precisions of
150 ±1.5 (1-h average) and ±0.5 µg/m³. The models used in the network are TEOM 1400a and TEOM
151 1405, and the entire system was heated to 50 °C; thus, a loss of semivolatile compounds cannot be
152 avoided. Our previous study showed that up to 25% lower mass concentrations were found for select
153 daily means than those observed with gravimetric filter measurements, depending on the
154 ammonium-nitrate levels and ambient temperatures (Liu et al., 2015). The errors of the TEOM
155 measurements are systematic in that they are always negative. Thus, these errors may not be
156 important for the study of the spatial distributions and temporal variations of PM_{2.5}. The other six
157 sites of the network were equipped with beta gauge instruments (EBAM, Met One Instruments Inc.,
158 Oregon) (Table S1). The measurement range of EBAM is 0-1000 µg/m³, with a precision of 0.1
159 µg/m³ and a resolution of 0.1 µg/m³. The filters were changed every week, and the inlet was cleaned
160 every month. The flow rates were also monitored and concurrently calibrated.

161 **2.3 Filter sampling and chemical analysis**

162 In this study, filter sampling was conducted at the five urban sites of Beijing, Guangzhou, Lhasa,
163 Shenyang and Chongqing as well as at the six background sites of Xinglong, Lin'an, Dinghu
164 Mountain, Namsto, Changbai Mountain and Gongga Mountain. The Automatic Cartridge Collection
165 Unit (ACCU) system of Rupprecht & Patashnick Co. with 47 mm diameter quartz fiber filters (Pall
166 Life Sciences, Ann Arbor, MI, USA) was deployed in Beijing to collect the PM_{2.5} samplers (Liu et
167 al., 2016a). Similar to the ACCU system, a standard 47 mm filter holder with quartz fiber filters
168 (Pall Life Sciences, Ann Arbor, MI, USA) was placed in the bypass line of TEOM 1400a and TEOM



169 1405 using quick-connect fittings and was used to collect the PM_{2.5} samplers of the other nine sites,
170 excepting Guangzhou and Lin'an. Each set of the PM_{2.5} samples was continuously collected over 48
171 h on the same days of each week, generally starting at 8:00 a.m. The flow rates were typically
172 15.6 L/min. For the Guangzhou site, the fine particles were collected on Whatman quartz fiber filters
173 using an Andersen model SA235 sampler (Andersen Instruments Inc.) with an air flow rate of
174 1.13 m³/min. The sampling lasted 24 or 48 h, generally starting at 8:00 a.m. For the Lin'an site, a
175 medium volume PM_{2.5} sampler (Model: TH-150CIII, Tianhong Instrument CO., Ltd. Wuhan, China)
176 was used to collect 24 h of PM_{2.5} aerosols on 90 mm quartz fiber filters (QMA, Whatman, UK) once
177 every 6 days (Xu et al., 2017). The sampling periods of these 11 urban and background sites are
178 shown in Table S1.

179 All the filters were heat treated at 500 °C for at least 4 h for cleaning prior to filter sampling.
180 The PM_{2.5} mass concentrations were obtained via the gravimetry method with an electronic balance
181 with a detection limit of 0.01 mg (Sartorius, Germany) after stabilizing at a constant temperature
182 (20±1 °C) and humidity (45%±5%). Three types of chemical species were measured using the
183 methods described in Xin et al. (2015). Briefly, the OC and elemental carbon (EC) values were
184 determined using a thermal/optical reflectance protocol using a DRI model 2001 carbon analyzer
185 (Atmoslytic, Inc., Calabasas, CA, USA). Eight main ions, including K⁺, Ca²⁺, Na⁺, Mg²⁺, NH₄⁺,
186 SO₄²⁻, NO₃⁻ and Cl⁻, were measured via ion chromatography (using a Dionex DX 120 connected to
187 a DX AS50 autosampler for anions and a DX ICS90 connected to a DX AS40 autosampler for
188 cations), and 18 elements, including Mg, Al, K, Ca, V, Cr, Mn, Fe, Co, Ni, Cu, Zn, As, Se, Ag, Cd,
189 Tl and Pb, were determined by Agilent 7500a inductively coupled plasma mass spectrometry (ICP-
190 MS, Agilent Technologies, Tokyo, Japan).

191

192 3. Results and discussions

193 3.1 Characteristics of PM_{2.5} mass concentrations at urban and background sites

194 3.1.1 Average PM_{2.5} levels

195 The location, station information and average PM_{2.5} concentrations from the 40 monitoring
196 stations are shown in Fig. 1 and Table 1. The highest PM_{2.5} concentrations were observed at the
197 urban stations of Xi'an (125.8 µg/m³), Taiyuan (111.5 µg/m³), Ji'nan (107.5 µg/m³) and Shijiazhuang
198 (105.1 µg/m³), which are located in the most polluted areas of the Guanzhong Plain (GZP) and the
199 North China Plain (NCP). Several studies have revealed that the enhanced PM_{2.5} pollutions of the
200 GZP and NCP are not only due to the primary emissions from local sources such as the local
201 industrial, domestic and agricultural sources but are also due to secondary productions (Huang et
202 al., 2014; Guo et al., 2014; Wang et al., 2014). Furthermore, the climates of the GZP and NCP are
203 characterized by stagnant weather with weak winds and relatively low boundary layer heights,
204 leading to favorable atmospheric conditions for the accumulation, formation and processing of
205 aerosols (Chan and Yao, 2008). Note that the averaged PM_{2.5} concentrations in Beijing and Tianjin
206 were approximately 70 µg/m³, which is much lower than those of the other cities, including Ji'nan
207 and Shijiazhuang in the NCP, possibly because Beijing and Tianjin are located in the northern part
208 of the NCP, far from the intense industrial emission area that is mainly located in the southern part
209 of the NCP. Interestingly, the average PM_{2.5} concentrations at Yucheng (102.8 µg/m³) and Xianghe
210 (83.7 µg/m³) were even higher than most of those from the urban stations. Although Yucheng is a



211 rural site, it is located in an area with rapid urbanization near Ji'nan and is therefore subjected to the
212 associated large quantities of air pollutants. In addition, Xianghe is located between Beijing and
213 Tianjin and is influenced by the regionally transported contributions from nearby megacities and
214 the primary emissions from local sources. Yantai is a coastal city with relatively low PM
215 concentrations compared to those of with inland cities on the NCP.

216 The PM_{2.5} concentrations were also high in the Yangtze River Delta (YRD), which is another
217 developed and highly-populated city cluster area like the NCP (Fu et al., 2013). The average PM_{2.5}
218 values of the three urban stations of Shanghai, Wuxi and Hefei were 56.2, 65.2 and 80.4 µg/m³,
219 respectively, which are comparable to those of the megacities of Beijing and Tianjin in the NCP.
220 Due to the presence of fewer coal-based industries and dispersive weather conditions, the PM_{2.5}
221 concentrations of the Pearl River Delta (PRD) are generally lower than those of the other two largest
222 city clusters in China, such as those from the NCP and YRD. The average PM_{2.5} value at Guangzhou
223 was 44.1 µg/m³, which was similar to the PM_{2.5} values of the background stations from the NCP and
224 YRD. Shenyang, the capital of the province of Liaoning, is located in the Northeast China Region
225 (NECR), which is an established industrial area. High concentrations of trace gases and aerosol
226 scattering in the free troposphere have been observed via aircraft observations and are due to
227 regional transports and heavy local industrial emissions (Dickerson et al., 2007). In the present study,
228 the average PM_{2.5} concentration of Shenyang was 77.6 µg/m³. Meanwhile, Hailun, which is a rural
229 site in northeastern China, had an average PM_{2.5} concentration of 41.6 µg/m³, which was much
230 lower than that of the rural site of Yucheng in the NCP.

231 High aerosol optical depths and low visibilities have been observed in the Sichuan Basin
232 (Zhang et al., 2012), which is located in the Southwestern China Region (SWCR). The poor
233 dispersion conditions and heavy local industrial emissions make this another highly polluted area in
234 China. In the present study, the average PM_{2.5} concentration in Chengdu was measured as 102.2
235 µg/m³, which is much higher than the averages from the megacities of Beijing, Shanghai and
236 Guangzhou but is comparable to those of Ji'nan and Shijiazhuang. Chongqing, another megacity
237 located in the SWCR, however, showed much lower PM_{2.5} values than Chengdu. Urumqi, the capital
238 of the Uighur Autonomous Region of Xinjiang, located in northwestern China, experiences air
239 pollution due to its increasing consumption of fossil fuel energy and steadily growing fleet of motor
240 vehicles (Mamtimin and Meixner, 2011). The average PM_{2.5} concentration measured in Urumqi is
241 104.1 µg/m³, which is comparable to those of the urban sites in the GZP and NCP. The similarity
242 among the PM_{2.5} values for Cele, Dunhuang and Fukang is due to their location, being far from
243 regions with intensive economic development but strongly affected by sandstorms and dust storms
244 due to their proximity to dust source areas. For example, the average PM_{2.5} concentration in Cele
245 during the spring (200.7 µg/m³) was much greater than those of the other three seasons. Lhasa, the
246 capital of the Tibet Autonomous Region (TAR), is located in the center of the Tibetan Plateau at a
247 very high altitude of 3700 m. The PM_{2.5} concentrations in Lhasa were low, with average values of
248 30.6 µg/m³, because of its relatively small population and few industrial emissions.

249 Much lower PM_{2.5} concentrations were observed at the background stations, the values of
250 which ranged from 11.2 to 46.5 µg/m³. The lowest concentration of PM_{2.5} was observed in Namsto,
251 a background station on the TAR with nearly no anthropogenic effects. The highest PM_{2.5}
252 concentration of the background stations was observed at Lin'an, a background station in the PRD.



253 The average $PM_{2.5}$ concentration at the urban and background sites in this study are shown as box-
254 plots in Fig. S1a. The average $PM_{2.5}$ concentration of the background stations (a total of 12 sites) is
255 $28.5 \mu\text{g}/\text{m}^3$, and the average concentration of the $PM_{2.5}$ values from urban stations (a total of 20
256 sites) is $73.2 \mu\text{g}/\text{m}^3$. The latter value is approximately three times the former, suggesting the large
257 differences in fine particle pollution at urban and background sites across China. All values were
258 much greater than the results from Europe and North America. Gehrig and Buchmann (2003)
259 reported that average $PM_{2.5}$ concentrations from 1998 to 2001 at urban/suburban stations in
260 Switzerland were $20.1 \mu\text{g}/\text{m}^3$. The average $PM_{2.5}$ concentrations were $16.3 \mu\text{g}/\text{m}^3$ for the period
261 2008-2009 in the Netherlands (Janssen et al., 2013). Between October 2008 and April 2011, the 20
262 study areas of the European ESCAPE project showed annual average concentrations of $PM_{2.5}$
263 ranging from 8.5 to $29.3 \mu\text{g}/\text{m}^3$, with low concentrations in northern Europe and high concentrations
264 in southern and eastern Europe (Eeftens et al., 2012). An average $PM_{2.5}$ value of $14.0 \mu\text{g}/\text{m}^3$ was
265 observed over the study period of 2000-2005 via measurements from 187 counties in the United
266 States, with higher values in the eastern United States and California and lower values in the central
267 regions and the northwest (Bell et al., 2007).

268 To further characterize these kinds of differences for different parts of China, six pairs of $PM_{2.5}$
269 values measured from urban and background stations were selected to represent the NCP, YRD,
270 PRD, TAR, NECR and SWCR, respectively (Fig. S1). The first three areas (NCP, YRD and PRD)
271 and the last two areas (NECR and SWCR) were the most industrialized and populated regions in
272 China, while TAR is the cleanest area in China. The $PM_{2.5}$ concentrations of the background stations
273 in the NCP, YRD and PRD are $39.8 \mu\text{g}/\text{m}^3$ (Xinglong), $46.5 \mu\text{g}/\text{m}^3$ (Lin'an) and $40.1 \mu\text{g}/\text{m}^3$ (Dinghu
274 Mountain) and are much higher than those of the background stations in other parts of China, which
275 are usually below $25 \mu\text{g}/\text{m}^3$. In addition, the background $PM_{2.5}$ concentrations in the NCP, YRD and
276 PRD were comparable to those from nearby urban sites, especially for the PRD, as shown in Fig.
277 S1. In contrast, the background $PM_{2.5}$ concentrations in TAR, NECR and SWCR were much lower
278 than those of the nearby cities. These results suggest that the background sites in the NCP, YRD and
279 PRD are more influenced by regional pollution, which will be further discussed in section 3.2.

280 3.1.2 Seasonal variations of $PM_{2.5}$ mass concentrations

281 Generally, the $PM_{2.5}$ concentrations in urban areas show distinct seasonal variabilities, with
282 maxima during the winter and minima during the summer for most of China (Fig. 1), which is a
283 similar pattern to that of the results reported by Zhang and Cao (2015). In northern and northeastern
284 China, the wintertime peak values of $PM_{2.5}$ were mainly attributed to the combustion of fossil fuels
285 and biomass burning for domestic heating over extensive areas, which emit large quantities of
286 primary particulates as well as the precursors of secondary particles (He et al., 2001). In addition,
287 new particle formation and the secondary production of both inorganic aerosols and OM could
288 further enhance fine PM abundance (Huang et al., 2014; Guo et al., 2014). Furthermore, the
289 planetary boundary layer is relatively low in the winter, and more frequent occurrences of stagnant
290 weather and intensive temperature inversions cause very bad diffusion conditions, which can result
291 in the accumulation of atmospheric particulates and lead to high-concentration PM episodes (Quan
292 et al., 2014; Zhao et al., 2013b). In southern and eastern China, although the effect of domestic
293 heating is not as important as that in northern China, the weakened diffusion and transport of
294 pollutants from the north due to the activity of the East Asian Winter Monsoon reinforces the



295 pollution from large local emissions in the winter more than in any other season (Li et al., 2011;
296 Mao et al., 2017). For northwestern and West Central China, the most polluted season is the spring
297 instead of the winter due to the increased contribution from dust particles in this desert-like region
298 (Zou and Zhai, 2004), suggesting that the current PM_{2.5} control strategies (i.e., reducing fossil/non-
299 fossil combustion derived VOCs and PM emissions) will only partly reduce the PM_{2.5} pollution in
300 western of China. PM_{2.5} is greatly decreased during the summer in urban areas, which is associated
301 with the reduced anthropogenic emissions from fossil fuel combustion and biomass burning
302 domestic heating. Further, the more intense solar radiation causes a higher atmospheric mixing layer,
303 which leads to strong vertical and horizontal aerosol dilution effects (Xia et al., 2006). In addition,
304 increased precipitation in most of China due to the summer monsoon can increase the wet
305 scavenging of atmospheric particles. As a result, PM_{2.5} minima are observed in the summer at urban
306 sites.

307 The seasonal variations of PM_{2.5} at the background sites varied in different parts of China
308 (Fig. 3). Dinghu Mountain and Lin'an showed maximum values in the winter, while Zangdongnan,
309 Qinghai Lake, Xishuangbanna and Mount Everest showed maximum values in the spring. In
310 addition, a summer maximum of PM_{2.5} was observed for Xinglong, and an autumn maximum was
311 observed for Tongyu. Changbai Mountain, Gongga Mountain and Namsto showed weak seasonal
312 variabilities. These results suggest the different contributions from regional anthropogenic and
313 natural emissions and long-range transports to background stations. The monthly average PM_{2.5}
314 concentrations of the urban and background sites in the NCP, YRD, PRD, TAR, NECR and SWCR
315 are further analyzed and shown in Fig. 2. The monthly variations of the PM_{2.5} concentrations at the
316 background sites in the YRD and PRD were consistent with those of the nearby urban sites, both of
317 which showed maximum values in December (YRD) and January (PRD). The reasons for this
318 similarity are primarily the seasonal fluctuations of emissions, which are already well known due to
319 the similar variations of other parameters, including sulfur dioxide and nitrogen oxide, as shown in
320 Fig. S2. In contrast, the monthly variations of PM_{2.5} at Xinglong showed different trends than those
321 of the nearby urban stations. The maximum value of PM_{2.5} at this site was observed in July, while
322 the maximum value in Beijing was observed in January. The reasons for this are not primarily the
323 seasonal fluctuations of emissions, but rather meteorological effects (frequent inversions during the
324 winter and strong vertical mixing during the summer). The Xinglong site is situated at an altitude of
325 900 m a.s.l., and therefore, during the wintertime, the majority of cases above the inversion layer
326 are protected from the emissions of the urban agglomerations of the NCP. Furthermore, in the NCP
327 area, northerly winds prevail in the winter, while southerly winds prevail in the summer. Thus, in
328 the summer, more air masses from the southern urban agglomerations will lead to high PM_{2.5}
329 concentrations in Xinglong. Weak monthly variabilities were observed for Namsto, Changbai
330 Mountain and Gongga Mountain, although remarkable monthly variabilities were found at the
331 nearby cities of Lhasa, Shenyang and Chongqing. The reasons for this difference are mainly that
332 these three sites are elevated remote stations that are far from human activities and show
333 predominant meteorological influences.

334 3.1.3 Diurnal variations of PM_{2.5} mass concentrations

335 To derive importance information to identify the potential emission sources and the times
336 when the pollution levels exceed the proposed standards, hourly data were used to examine the



337 diurnal variabilities of $PM_{2.5}$ as well as those of the other major air pollutants. Fig. 3 illustrates the
338 diurnal variations of the hourly $PM_{2.5}$ concentrations in Beijing, Shanghai, Guangzhou, Lhasa,
339 Shenyang and Chongqing, in the largest megacities in the NCP, YRD, PRD, TPR, NECR and SWCR
340 and in the different climatic zones of China, respectively. Of the urban sites, Lhasa has the lowest
341 $PM_{2.5}$ concentrations, but the most significant pronounced diurnal variations of $PM_{2.5}$, with obvious
342 morning and evening peaks appearing at 10:00 and 22:00 (Beijing Time) due to the contributions of
343 enhanced anthropogenic activity during the rush hours. The minimum value occurred at 16:00,
344 which is mainly due to a higher atmospheric mixing layer, which is beneficial for air pollution
345 diffusion. This bimodal pattern was also observed in Shenyang and Chongqing, which show
346 morning peaks at 7:00 and 9:00 and evening peaks at 19:00 and 20:00, respectively. However, the
347 $PM_{2.5}$ values in Beijing, Shanghai and Guangzhou showed much weaker urban diurnal variation
348 patterns, and slightly higher $PM_{2.5}$ concentrations during the night than during the day were
349 observed, which can be explained by the enhanced emissions from heating and the relatively low
350 boundary layer. Note that the morning peaks in Beijing, Shanghai and Guangzhou were not as
351 obvious as those of other cities, although both the SO_2 and NO_2 values increased due to increased
352 anthropogenic emissions (Fig. S3). Alternatively, this decreasing trend may be the result of an
353 increasing boundary layer depth. At these three urban sites, the $PM_{2.5}$ levels started to increase in
354 the late afternoon, which could be explained by the increasing motor vehicle emissions as NO_2 is
355 also dramatically increased during the same period.

356 At the background area of the TPR, significant pronounced diurnal variations of $PM_{2.5}$ were
357 observed in Namsto, with a morning peak at 9:00 and an evening peak at 21:00 (Fig. 3d), which are
358 similar to those of the urban site of Lhasa. As there are hardly any anthropogenic activities near
359 Namsto, this kind of diurnal pattern of $PM_{2.5}$ may be influenced by the evolution of the planetary
360 boundary layer. Both Lin'an and Gongga Mountain showed the same bimodal pattern of $PM_{2.5}$ as
361 that in Namsto, which could also be influenced by the planetary boundary layer. For the background
362 site of the NCP, however, Xinglong showed smooth $PM_{2.5}$ variations. As mentioned before, the
363 Xinglong station is located on the mountain and has an altitude of 960 m a.s.l. The mixed boundary
364 layer of the urban area increases in height in the morning and reaches a height of approximately
365 1000 meters in the early afternoon. Then, the air pollutants from the urban area start to affect the
366 station as the vertical diffusion of the airflow and the $PM_{2.5}$ concentration reach their maxima at
367 18:00. Next, the concentration starts to decrease when the mixed boundary layer collapses in the
368 late afternoon, eventually forming the nocturnal boundary layer (Boyok et al., 2010). Thus, $PM_{2.5}$
369 concentration decreased slowly during the night and morning, reaching a minimum at 10:00. At
370 Dinghu Mountain and Changbai Mountain, the daytime $PM_{2.5}$ greater than that of the nighttime,
371 with a maximum value occurring at approximately 11:00-12:00. This kind of diurnal pattern of
372 $PM_{2.5}$ is mainly determined by the effects of the mountain-valley breeze. Both the Dinghu Mountain
373 and Changbai Mountain stations are located near the mountain. Thus, during daytime, the valley
374 breeze from urban areas carries air pollutants that will accumulate in front of the mountain and cause
375 an increase of the PM concentration. Meanwhile, at night, the fresh air carried by the mountain
376 breeze will lead to the dilution of the PM, so low concentrations are sustained during the night.
377 Further support for this pattern comes from the much higher maximum values of $PM_{2.5}$ in the winter
378 than those in the summer, as enhanced air pollutant emissions in urban areas are expected in the



379 winter due to heating.

380 **3.2 Chemical compositions of PM_{2.5} in urban and background sites**

381 **3.2.1 Overview of PM_{2.5} mass speciation**

382 Figure 4 shows the annual average and seasonal average chemical compositions of PM_{2.5} at
383 six urban and six background sites, which represent the largest megacities and regional background
384 areas of the NCP, YRD, PRD, TPR, NECR and SWCR. The chemical species of PM_{2.5} in Shanghai
385 were obtained from Zhao et al. (2015). The atmospheric concentrations of the main PM_{2.5}
386 constituents are also shown in Table 2. The EC, nitrate (NO₃⁻), sulfate (SO₄²⁻), ammonium (NH₄⁺)
387 and chlorine (Cl⁻) concentrations were derived directly from measurements. Organic matter (OM)
388 was calculated assuming an average molecular weight per carbon weight, showing an OC of 1.6 at
389 the urban sites and of 2.1 at the background sites, based on the work of Turpin and Lim (2001);
390 however, these values are also spatially and temporally variable, and typical values could range from
391 1.3 to 2.16 (Xing, et al., 2013). The calculation of mineral dust was performed on the basis of crustal
392 element oxides (Al₂O₃, SiO₂, CaO, Fe₂O₃, MnO₂ and K₂O). In addition, the Si content, which was
393 not measured in this study, was calculated based on its ratio to Al in crustal materials; namely,
394 [Si]=3.41×[Al]. Finally, the unaccounted-for mass refers to the difference between the PM_{2.5}
395 gravimetric mass and the sum of the PM constituents mentioned above.

396 The PM constituents' relative contributions to the PM mass are independent of their dilutions
397 and reflect differences in the sources and processes controlling the aerosol compositions (Putaud et
398 al., 2010). When all the main aerosol components except water are quantified, they account for 73.6-
399 84.8% of the PM_{2.5} mass (average 79.2%) at urban sites and for 76.2-91.1% of the PM_{2.5} mass
400 (average 83.4%) at background sites. The remaining unaccounted-for mass fraction may be the
401 result of analytical errors, a systematic underestimation of the PM constituents whose concentrations
402 are calculated from the measured data (e.g., OM, and mineral dust), and aerosol-bound water
403 (especially when mass concentrations are determined at RH >30%). For the urban sites, the mean
404 composition given in descending concentrations is 26.0% OM, 17.7% SO₄²⁻, 11.8% mineral dust,
405 9.8% NO₃⁻, 6.6% NH₄⁺, 6.0% EC and 1.2% Cl⁻. For the background sites, the mean composition
406 given in descending concentrations is 33.2% OM, 17.8% SO₄²⁻, 10.1% mineral dust, 8.7% NH₄⁺,
407 8.6% NO₃⁻, 4.1% EC and 0.9% Cl⁻. Generally, the chemical compositions of the PM_{2.5} at background
408 sites are similar to those of the urban sites, although they show a much higher fraction of OM and
409 lower fractions of NO₃⁻ and EC. Significant seasonal variations of the chemical compositions were
410 observed at urban sites (Fig. 4c), with much higher fractions of OM (33.7%) and NO₃⁻ (11.1%) in
411 the winter and much lower fractions of OM (20.7%) and NO₃⁻ (6.9%) in the summer. In contrast,
412 the fraction of SO₄²⁻ was consistent among the different seasons, although its absolute concentration
413 in the winter (14.9 µg/m³) was higher than that in the summer (11.7 µg/m³). Compared with those
414 at urban sites, different seasonal variation of OM were observed at the background sites, which
415 showed summer maxima and winter/spring minima (Fig. 4d). While the wintertime peaks of OM at
416 the urban sites were probably due to additional local emissions sources related to processes like
417 heating, the summer peaks at the background sites were attributed to the enhanced biogenic
418 emissions. Note that the seasonal variations of NO₃⁻ were similar to those at urban sites; this seasonal
419 phenomenon is due to the favorable conditions of cold temperature and high relative humidity
420 conditions leading to the formation of particulate nitrate. The seasonal behaviors of SO₄²⁻ at the



421 background sites were markedly different than those of the urban sites and indicate very different
422 sources and atmospheric processing of SO_4^{2-} , which will be further discussed for specific regions of
423 China.

424 There are significant variations of the absolute speciation concentrations at these urban and
425 background sites (Table 2). For the urban sites, the OM concentrations span a 2-fold concentration
426 range from $12.6 \mu\text{g}/\text{m}^3$ (Lhasa) to $23.3 \mu\text{g}/\text{m}^3$ (Shenyang), while these values range from $3.4 \mu\text{g}/\text{m}^3$
427 (Namtso) to $21.7 \mu\text{g}/\text{m}^3$ (Lin'an) at the background sites. The SO_4^{2-} and NO_3^- concentrations exhibit
428 larger spatial heterogeneities than those of the OM for both urban and background sites. The
429 absolute values of SO_4^{2-} have an approximately 25-fold range in urban sites, from $0.8 \mu\text{g}/\text{m}^3$ (Lhasa)
430 to $19.7 \mu\text{g}/\text{m}^3$ (Chongqing), while this value has a 30-fold range at the background sites, from 0.4
431 $\mu\text{g}/\text{m}^3$ (Namtso) to $11.2 \mu\text{g}/\text{m}^3$ (Lin'an). The corresponding mass fractions are 26.8% in Chongqing
432 and below 3% in Lhasa. Much higher fractions of SO_4^{2-} in the $\text{PM}_{2.5}$ were observed at the urban sites
433 located in southern China than those in northern China, although the average concentration of $\text{PM}_{2.5}$
434 is greater in the north than in the south, suggesting that sulfur pollution remains a problem for
435 southern China (Liu, et al., 2016b). This problem may be attributed to higher sulfur contents of the
436 coal in southern China, with 0.51% in the north vs. 1.32% in the south and up to >3.5% in Chongqing
437 in southern China (Lu et al., 2010; Zhang et al., 2010). The absolute values of NO_3^- have an
438 approximately 20-fold range in urban sites and a greater than 100-fold range in background sites.
439 This heterogeneity reflects the large spatial and temporal variations of the NO_x sources. For the
440 urban sites, the absolute EC values have a 5-fold concentration range, from $1.4 \mu\text{g}/\text{m}^3$ (Lhasa) to
441 greater than $7.0 \mu\text{g}/\text{m}^3$ (Guangzhou), while this species has a 15-fold concentration range at the
442 background sites and is mainly from anthropogenic sources. In comparison, the absolute
443 concentrations of mineral dust exhibit much weaker spatial variations at the urban and background
444 sites.

445 The characteristics of the $\text{PM}_{2.5}$ chemical compositions at individual site were discussed in
446 more detail. In this section, six pairs of urban and background sites from each region of China were
447 selected, and the differences in the chemical compositions of urban and background sites were
448 analyzed.

449 3.2.2 North China Plain

450 Beijing is the capital of China and has attracted considerable attention due to its air pollution
451 (Chen et al., 2013). Beijing is the largest megacity in the NCP, which is surrounded by the Yanshan
452 Mountains to the west, north and northeast and is connected to the Great North China Plain to the
453 south. The filter sampler is located in the courtyard of the Institute of Atmospheric Physics (IAP)
454 (116.37°E , 39.97°N), 8 km northwest of the center of downtown. The $\text{PM}_{2.5}$ concentration during
455 the filter sampling period was $71.7 \mu\text{g}/\text{m}^3$, which is close to the three-year average $\text{PM}_{2.5}$ value
456 reported by TEOM (Table 1). $\text{PM}_{2.5}$ in Beijing is mainly composed by OM (26.6%), SO_4^{2-} (16.5%)
457 and NO_3^- (13.0%) (Fig. 5a), which compare well with previous studies (Yang et al., 2011; Oanh et
458 al., 2006). However, the mineral dust fraction found in this study (6.5%) was much lower than that
459 found in Yang et al. (2011) (19%) but was comparable to that found in Oanh et al. (2006) (5%),
460 potentially due to difference in definitions. The annual concentration of OM ($19.1 \mu\text{g}/\text{m}^3$) in Beijing
461 was comparable to those in Shanghai, Guangzhou and Chongqing, but was much lower than that in
462 Shenyang. Higher fractions of OM were observed in the winter (34.2%) and autumn (30.5%) than



463 in the summer (21.6%) and spring (20.9%). The annual concentration of SO_4^{2-} ($11.9 \mu\text{g}/\text{m}^3$) was
464 much lower than those of earlier years ($15.8 \mu\text{g}/\text{m}^3$, 2005-2006) (Yang et al., 2011), suggesting that
465 the energy structure adjustment implemented in Beijing (e.g., replacing coal fuel with natural gas)
466 has been effective in decreasing the particulate sulfate in Beijing. Further support for this comes
467 from the SO_4^{2-} concentration in the winter ($16.5 \mu\text{g}/\text{m}^3$) being comparable to that in the summer
468 ($13.4 \mu\text{g}/\text{m}^3$). The significant NO_3^- value ($9.3 \mu\text{g}/\text{m}^3$) reflects the significant urban NO_x emissions
469 in Beijing, which was greatest during the winter, as expected from ammonium-nitrate
470 thermodynamics. The greater mineral component in the spring reflects the regional natural dust
471 sources.

472 The filter sampling site in Xinglong (117.58°E , 40.39°N) was located at Xinglong Observatory,
473 National Astronomical Observatory, Chinese Academy of Sciences, which is 110 km northeast of
474 Beijing (Fig. 1). This site is surrounded by mountains and is minimally affected by anthropogenic
475 activities. The $\text{PM}_{2.5}$ concentration during the filter sampling period was $42.6 \mu\text{g}/\text{m}^3$, which is close
476 to the three-year average $\text{PM}_{2.5}$ values reported by TEOM (Table 1). The annual chemical
477 composition of the $\text{PM}_{2.5}$ in Xinglong was similar to that in Beijing, although relatively higher
478 fractions of OM and sulfate were observed in Xinglong (Fig. 5a). Higher fractions of OM were
479 found in the winter (36.7%), and higher fractions of sulfate were found in the summer (32.1%) than
480 in any other season (OM: 23.0-30.4%; SO_4^{2-} : 15.7-20.1%). Interestingly, the summer SO_4^{2-}
481 concentration in Xinglong ($14.4 \mu\text{g}/\text{m}^3$) was even higher than that in Beijing, suggesting spatially
482 uniform distributions of SO_4^{2-} concentrations across the NCP. This result indicates that regional
483 transport can be an important source of SO_4^{2-} aerosols in Beijing, especially during the summer.

484 3.2.3 Yangtze River Delta

485 Shanghai is the economic center of China, lying on the edge of the broad flat alluvial plain of
486 the YRD, with a few mountains to the southwest. The filter sampler was located at the top of a four-
487 floor building of the East China University of Science and Technology (121.52°E , 31.15°N) (Zhao
488 et al., 2015), approximately 10 km northwest of the center of downtown. The $\text{PM}_{2.5}$ concentration
489 during the filter sampling period was $68.4 \mu\text{g}/\text{m}^3$, which is greater than the three-year average $\text{PM}_{2.5}$
490 value reported by EBAM, likely due to the different sampling period (Table S1). The $\text{PM}_{2.5}$ in
491 Shanghai mainly comprises OM (24.9%), SO_4^{2-} (19.9%) and NO_3^- (17.4%), which is comparable to
492 the results of previous studies (Ye et al., 2003; Wang et al., 2016). This site had the highest NO_3^-
493 ($11.9 \mu\text{g}/\text{m}^3$) and the second-highest SO_4^{2-} ($13.6 \mu\text{g}/\text{m}^3$) values of the urban sites, while its OM (17.1
494 $\mu\text{g}/\text{m}^3$) was comparable to those of Guangzhou and Chongqing. The SO_4^{2-} and NO_3^- values were
495 highest during the autumn as expected based on the widespread biomass burning in the autumn in
496 the YRD (Niu et al., 2013). However, the OM values were highest during the winter and mainly
497 originated from secondary aerosol processes based on the highest OC/EC ratios (6.0) and the poor
498 relationship of the OC and EC in this season.

499 Filter sampling was conducted at the Lin'an Regional Atmospheric Background Station
500 (119.73°E , 30.30°N), which is a background monitoring station for the World Meteorological
501 Organization (WMO) global atmospheric observation network. The Lin'an site was located at the
502 outskirts of Lin'an County within Hangzhou Municipality, which was 200 km southwest of
503 Shanghai (Fig. 1). This site is surrounded by agricultural fields and woods and is less affected by
504 urban, industrial and vehicular emissions (Xu et al., 2017). The $\text{PM}_{2.5}$ concentration during the filter



505 sampling period was $66.3 \mu\text{g}/\text{m}^3$, which is higher than the three-year average $\text{PM}_{2.5}$ values reported
506 by TEOM, likely due to the different sampling period (Table S1). The annual chemical composition
507 of the $\text{PM}_{2.5}$ in Lin'an was different than that in Shanghai, with much higher fractions of OM (32.7%)
508 and NH_4^+ (11.0%). Furthermore, the absolute concentration of OM in Lin'an was much higher than
509 that in Shanghai, especially in the summer (21.7 vs. $9.9 \mu\text{g}/\text{m}^3$), which may be attributed to the
510 enhanced biomass burning at both local and regional scales as well as the higher concentration of
511 summer EC in Lin'an than in Shanghai (2.2 vs. $1.4 \mu\text{g}/\text{m}^3$). In addition, the SO_4^{2-} and NO_3^-
512 concentrations in Lin'an were comparable to those in Shanghai. These results suggest a spatially
513 homogeneous distribution of secondary aerosols over the PRD and the transportation of aged
514 aerosol and gas pollutants from city clusters has significantly changed the aerosol chemistry in the
515 background area of this region.

516 3.2.4 Pearl River Delta

517 Guangzhou is the biggest megacity in south China located in the PRD and mainly consists of
518 floodplains within the transitional zone of the East Asian monsoon system (Yang et al., 2011). The
519 filter sampler was set up on the rooftop of a 15-m high building of the Guangzhou Institute of
520 Geochemistry, Chinese Academy of Sciences (113.35°E , 23.12°N). This site was surrounded by
521 heavily trafficked roads and dense residential areas, representing a typical urban location. The $\text{PM}_{2.5}$
522 concentration during the filter sampling period was $75.3 \mu\text{g}/\text{m}^3$, which is much higher than the three-
523 year average $\text{PM}_{2.5}$ value reported by EBAM (Table 1), likely due to the different sampling period
524 and location. The $\text{PM}_{2.5}$ in Guangzhou mainly comprises OM (22.2%), SO_4^{2-} (17.3%) and mineral
525 dust (9.7%), which have values comparable to previous studies conducted in the years of 2013-2014
526 (Chen et al., 2016; Tao et al., 2017). This site has the lowest OC/EC ratio (1.5) of all urban sites,
527 which can be explained by the abundance of diesel engine truck in Guangzhou City (Verma et al.,
528 2010). Obvious seasonal variations of OM, SO_4^{2-} and NO_3^- were observed, showing winter/autumn
529 maxima and summer/spring minima. In addition, summer minima were also observed for EC and
530 NH_4^+ . High mixing heights in the summer and clean air masses affected by summer monsoons from
531 the South China Sea should lead to the minima of these species in summer, while the low wind
532 speeds, weak solar radiation, relatively low precipitation (Tao et al., 2014) and relatively high
533 emissions (Zheng et al., 2009) result in the much higher concentrations of OM and secondary
534 inorganic aerosols (SO_4^{2-} , NO_3^- and NH_4^+) in the winter and autumn.

535 Filter sampling was conducted at Dinghu Mountain Station (112.50°E , 23.15°N), which is
536 located in the middle of Guangdong Province in southern China. This site was surrounded by hills
537 and valleys, being approximately 70 km west of Guangzhou (Fig. 1). The $\text{PM}_{2.5}$ concentration
538 during the filter sampling period was $40.1 \mu\text{g}/\text{m}^3$, close to the three-year average $\text{PM}_{2.5}$ values
539 reported by TEOM. Distinct seasonal variations of OM, SO_4^{2-} , NO_3^- and NH_4^+ were observed, with
540 the highest concentration of OM and NO_3^- occurring in the winter, while the highest concentrations
541 of SO_4^{2-} and NH_4^+ occurred in the autumn. In contrast, EC and mineral dust showed weak seasonal
542 variations. Dinghu Mountain has the second-highest EC and SO_4^{2-} values of the background sites,
543 being $2.0 \mu\text{g}/\text{m}^3$ and $10.1 \mu\text{g}/\text{m}^3$. In addition, the lowest OC/EC ratio was observed at Dinghu
544 Mountain (2.8); the other background sites had values ranging from 3.5-8.3. These results indicate
545 that this background site is intensely influenced by vehicular traffic, fossil fuel combustion and
546 industrial emissions due to the advanced urban agglomeration in the PRD region. These results are



547 consistent with the finds from previous studies (Liu et al., 2011; Wu et al., 2016). Compared with
548 those from Guangzhou, higher fractions of SO_4^{2-} and NO_3^- were observed at Dinghu Mountain,
549 while the fractions of OM and mineral dust were similar at these two sites, possibly indicating that
550 there was a significantly larger fraction of transported secondary aerosols or aged aerosols at the
551 background site of the PRD.

552 3.2.5 Tibetan Autonomous Region

553 Located in the inland TAR, Lhasa is one of the highest cities in the world (at an altitude of
554 3700 m). The city of Lhasa is located in a narrow west-east oriented valley in the southern part of
555 the TAR. The filter sampler was located on the roof of a 20-m high building on the campus of the
556 Institute of Tibetan Plateau Research (Lhasa branch) (91.63 E, 29.63 N). This site is close to Jinzhu
557 road, one of the busiest roads in the city (Cong et al., 2011). The $\text{PM}_{2.5}$ concentration during the
558 filter sampling period was $36.4 \mu\text{g}/\text{m}^3$, which is close to the three-year average $\text{PM}_{2.5}$ values reported
559 by TEOM. The $\text{PM}_{2.5}$ in Lhasa mainly comprises OM (34.5%) and mineral dust (31.9%), and the
560 secondary inorganic aerosols (SO_4^{2-} , NO_3^- and NH_4^+) contributed little to the $\text{PM}_{2.5}$ (<5%). These
561 results are comparable to those of a previous study conducted in the year of 2013-2014 (Wan et al.,
562 2016). In addition, this site reports the lowest OM ($12.6 \mu\text{g}/\text{m}^3$), secondary inorganic aerosols (1.7
563 $\mu\text{g}/\text{m}^3$) and EC ($1.4 \mu\text{g}/\text{m}^3$) values of the urban sites in this study. Higher fractions of OM were
564 observed in the winter (48.4%) and spring (43.1%), exceeding those in the summer (24.6%) and
565 autumn (31.2%). Weak seasonal variations were found for the SO_4^{2-} (1.5-3.0%) and NO_3^- (1.1-1.7%)
566 values, suggesting the negligible contributions from fossil fuel combustion in Lhasa.

567 Filter sampling was conducted at the Namtso Monitoring and Research Station for Multisphere
568 Interactions (90.98 E, 30.77 N), a remote site located on the northern slope of the Nyainqen-tanglha
569 Mountains, approximately 125 km northwest of Lhasa (Fig. 1). The $\text{PM}_{2.5}$ concentration during the
570 filter sampling period was $9.5 \mu\text{g}/\text{m}^3$, which is close to the three-year average $\text{PM}_{2.5}$ value reported
571 by TEOM. The $\text{PM}_{2.5}$ in Namtso mainly comprises mineral dust (40.8%) and OM (36.3%), while
572 SO_4^{2-} and NO_3^- contributed less than 5% to the $\text{PM}_{2.5}$. This chemical composition is distinctly
573 different from those of the other background sites in this study, but is comparable to the background
574 site at Qinghai Lake in the TAR (Zhang et al., 2014b). Namtso has the lowest OM, EC, SO_4^{2-} , NO_3^-
575 and NH_4^+ values of all the background sites in this study. Spring maxima and winter minima were
576 observed for the OM and EC, while the SO_4^{2-} , NO_3^- and NH_4^+ values showed weak seasonal
577 variations. The highest OC/EC ratio was observed (8.3) at this site, suggesting that the organic
578 aerosols at Namtso mainly originated from secondary aerosol processes or aged organic aerosols
579 from regional transports.

580 3.2.6 Northeast China Region

581 Shenyang is the capital city of Liaoning province and the largest city in northeastern China.
582 The main urban area is located on a delta to the north of the Hun River. The filter sampler was
583 located at the Shenyang Ecological Experimental Station of the Chinese Academy of Science
584 (123.40 E, 41.50 N) and was surrounded by residential areas with no obvious industrial pollution
585 sources around the monitoring station, representing the urban area of Shenyang. The $\text{PM}_{2.5}$
586 concentration during the filter sampling period was $81.8 \mu\text{g}/\text{m}^3$, which is close to the three-year
587 average $\text{PM}_{2.5}$ value reported by TEOM (Table 1). The $\text{PM}_{2.5}$ in Shenyang mainly comprises OM
588 (28.5%), SO_4^{2-} (16.1%) and mineral dust (11.3%). This site reports the highest OM ($23.3 \mu\text{g}/\text{m}^3$) and



589 mineral dust ($9.2 \mu\text{g}/\text{m}^3$) values as well as the second-highest EC ($5.2 \mu\text{g}/\text{m}^3$) value of the urban
590 sites. The NO_3^- concentration at this site, however, was the second-lowest of the urban sites (Table
591 2). Much higher fractions of OM were observed in the winter (40.5%) than in the other seasons
592 (15.6–26.5%) (Fig. 5), possibly due to the enhanced coal burning for winter heating. Further support
593 for this pattern comes from the high abundance of chlorine during the cold seasons, which is mainly
594 associated with coal combustion. The contribution from sea-salt particles is not important since the
595 sampling sites are at least 200 km from the sea. Note that the fraction of SO_4^{2-} in the $\text{PM}_{2.5}$ during
596 the winter was lower than that in the summer, although the absolute concentration was much higher
597 in the winter ($23.6 \mu\text{g}/\text{m}^3$) than in the summer ($11.3 \mu\text{g}/\text{m}^3$). This result may be attributed to the
598 reduced transformation of sulfur dioxide at low temperatures.

599 Filter sampling was conducted at the Changbai Mountain forest ecosystem station (128.01 E,
600 42.40 N), which was mostly surrounded by hills and forest and is located approximately 390 km
601 northeast of Shenyang (Fig. 1). This site is situated 10 km from the nearest town, Erdaobaihe, which
602 has approximately 45000 residents. The sources of PM were expected to be non-local. Hence, this
603 site is considered a background site in the NECR. The $\text{PM}_{2.5}$ concentration during the filter sampling
604 period was $23.3 \mu\text{g}/\text{m}^3$, which is close to the three-year average $\text{PM}_{2.5}$ value reported by TEOM
605 (Table 1). The main contributions to the $\text{PM}_{2.5}$ at Changbai Mountain were OM (38.1%), mineral
606 dust (16.0%) and SO_4^{2-} (14.3%), similar to those in Shenyang. Note that the summer OM
607 concentrations were quite similar at these two sites (8.0 vs. $9.0 \mu\text{g}/\text{m}^3$), but the OC/EC ratios were
608 different (4.8 vs. 1.6), which may reflect the different origins of the OM at the urban (primary
609 emissions) and background sites (secondary processes) of the NECR. The OM concentrations in the
610 other seasons were much lower at Changbai Mountain than those from Shenyang city, especially
611 during the winter (10.8 vs. $59.4 \mu\text{g}/\text{m}^3$). In fact, weak seasonal variations of chemical species (OM,
612 EC, SO_4^{2-} , NO_3^- and NH_4^+) were observed at Changbai Mountain. This site reports the second-
613 lowest values of OM, EC, SO_4^{2-} and Cl⁻ of the background sites. These results suggest that aerosols
614 at Changbai Mountain were influenced by the regional transports alone.

615 3.2.7 Southwestern China Region

616 Chongqing is the fourth municipality near Central China, lying on the Yangtze River in
617 mountainous southwestern China, near the eastern border of the Sichuan Basin and the western
618 border of Central China. For topographic reasons, Chongqing has some of the lowest wind speeds
619 in China (annual averages of $0.9\text{--}1.6 \text{ m s}^{-1}$ from 1979 to 2007; Chongqing Municipal Bureau of
620 Statistics, 2008), which favors the accumulation of pollutants. The filter sampler was located on the
621 rooftop of a 15-m high building on the campus of the Southwest University (106.54 E, 29.59 N).
622 This site is located in an urban district of Chongqing with no obvious industrial pollution sources
623 around the monitoring site, representing the urban area of Chongqing. The $\text{PM}_{2.5}$ concentration
624 during the filter sampling period was $73.5 \mu\text{g}/\text{m}^3$, of which 26.8% is SO_4^{2-} , 23.5% OM, 10.0%
625 mineral dust, 8.9% NO_3^- , 8.2% EC and 6.5% NH_4^+ . The OM fraction is smaller than those measured
626 by Yang et al. (2011) (32.7%) and Chen et al., 2017 (30.8%), while the SO_4^{2-} fraction is greater than
627 the values reported in these two studies (19.8–23.0%). This site shows the highest SO_4^{2-} ($19.7 \mu\text{g}/\text{m}^3$),
628 the highest NH_4^+ ($6.1 \mu\text{g}/\text{m}^3$) and the third-highest EC ($4.8 \mu\text{g}/\text{m}^3$) values of the urban sites. A weak
629 seasonal variation in the chemical composition of $\text{PM}_{2.5}$ was observed, although a much higher
630 concentration of this species was found in the winter than in the other seasons.



631 Filter sampling was performed at the Gongga Mountain Forest Ecosystem Research Station
632 (101.98 E, 29.51 N) in the Hailuoguo Scenic Area, a remote site located in southeastern Ganzi in
633 the Tibetan Autonomous Prefecture in Sichuan province. This site is mostly surrounded by glaciers
634 and forests and is located approximately 450 km northwest of Chongqing (Fig. 1). The PM_{2.5}
635 concentration during the filter sampling period was 32.2 µg/m³, close to the three-year average PM_{2.5}
636 value reported by TEOM (Table 1). The dominant components of PM_{2.5} were OM (40.7%), SO₄²⁻
637 (14.6%) and mineral dust (9.8%), similar to those at Changbai Mountain. This site has the second-
638 highest OM (13.1 µg/m³) value of the background sites, which may mainly be due to secondary
639 processes, considering the high OC/EC ratio (5.6). In addition, distinct seasonal variations of OM
640 were observed, which shows summer maxima (19.9 µg/m³) and autumn minima (9.1 µg/m³).
641 Previous studies showed higher mixing ratios of the VOCs during the spring and summer and lower
642 mixing ratios during the autumn at Gongga Mountain (Zhang et al., 2014c), which may result in
643 high concentrations of OM in the summer because the OC/EC ratio reaches its highest value in the
644 summer (10.3). Second-lowest EC and NO₃⁻ values of the background sites were observed here,
645 suggesting the insignificant influence of human activities in this region.

646 3.3 Temporal evolution and chemical composition PM_{2.5} in polluted days

647 Using the “Ambient Air Quality Standard” (GB3095-2012) of China (CAAQS), the
648 occurrences of polluted days exceeding the daily threshold values during 2012-2014 were counted
649 for each site (Fig. 6). Based on the number of polluted days exceeding the CAAQS daily guideline
650 of 35 µg/m³, substandard days of PM_{2.5} account for more than 60% of the total period at the majority
651 of urban sites, excepting Lhasa, Taipei and Sanya. Note that the ten most polluted cities (Ji'nan,
652 Chengdu, Taiyuan, Hefei, Shenyang, Xi'an, Changsha, Shijiazhuang, Wuxi and Chongqing)
653 experienced less than 20% clean days (daily PM_{2.5}<35 µg/m³) during the three-year observation
654 period. Interestingly, the occurrences of heavily polluted days (daily PM_{2.5}>150 µg/m³) were
655 different among these ten most polluted cities. While more than 15% of the total period comprised
656 heavily polluted days in Ji'nan, Taiyuan, Chengdu, Xi'an and Shijiazhuang, heavily polluted days
657 accounted for less than 5% of the total days in the other five cities, which mainly experienced
658 slightly polluted (35-75 µg/m³) and moderately polluted (75-115 µg/m³) days. Due to the regional
659 pollutant transports, the rural and background sites near the most polluted cities also showed high
660 occurrences of polluted days. Polluted days accounted for more than 50% of the total period at
661 Xin'long, Lin'an and Dinghu Mountain. In addition, an even higher occurrence of polluted days
662 (>80%) was found for the rural areas of Yucheng and Xianghe. In contrast, the background sites in
663 the TAR, NECR and SWCR rarely experienced polluted days, and over 80% of the total period
664 comprised clean days at these sites.

665 The polluted days were not equally distributed throughout the year. The monthly distributions
666 for the polluted days at each site are shown in Fig. 7. In terms of the occurrences of heavily polluted
667 days, December, January and February were predominant months for the urban sites located in the
668 most polluted areas of the GZP and NCP, where both the unfavorable dispersion conditions for
669 pollutants and the additional emission enhancements from residential heating contributed to the
670 heavy pollution in the winter. The heavy pollution occurring in April and November in Cele was
671 primarily caused by sandstorms and dust storms. Heavily polluted days were rarely observed at the
672 12 background sites in this study. The moderately polluted and polluted days were still mainly



673 concentrated in the winter in the megacities of the GZP and NCP and also occurred in the winter in
674 the megacities of the YRD and SWCR. In addition, March to June and September to October were
675 periods with high occurrences of polluted days. Dust storms from northern China (March to April),
676 biomass burning after crop harvests (May to June and September to October) and worsening
677 dispersion conditions after the summers likely accounted for the polluted days (Cheng et al., 2014;
678 Fu et al., 2014). The majority of slightly polluted days occurred from June to September, except at
679 several urban sites in southern China. The mass level of 35-75 $\mu\text{g}/\text{m}^3$ was considered a low level of
680 pollution for the entire year, illustrating that the summer and early autumn experienced cleaner
681 conditions.

682 The mean percentile compositions of the major components in $\text{PM}_{2.5}$ at different pollution
683 levels from four paired urban-background sites are shown in Fig. 8. With the pollution level
684 increased from clean to moderately polluted, the EC fraction in Beijing decreased slightly, the OM
685 fraction decreased significantly, and the sulfate and nitrate contributions increased sharply (Fig. 8a).
686 The same chemical evolution of the $\text{PM}_{2.5}$ was also observed at the background site of Xinglong,
687 suggesting that regional transport plays a vital role in the formation of the slightly and moderately
688 polluted days in the NCP. When the pollution level increased to heavily polluted, however, the OM
689 fraction further increased and was accompanied by increases of the sulfate and nitrate contributions
690 as well as decreases of the mineral dust contribution. This result indicates the enhanced secondary
691 transformation of gaseous pollutants (etc. SO_2 , NO_x , VOCs) during heavily polluted periods, which
692 is consistent with the findings of our previous study (Liu et al., 2016a), which stated that regionally
693 transported aerosols contribute the most during slightly and moderately polluted days, while local
694 origin secondary aerosols dominate the increases of fine particles during heavily polluted days in
695 Beijing. Unlike in Beijing, the contributions of OM and EC were almost constant across the different
696 pollution levels in Guangzhou, while the contribution of the secondary inorganic aerosols (SIA)
697 increased slightly (Fig. 8b). Interestingly, the nitrate contribution increased faster than that of the
698 sulfate when the pollution level increased from clean to heavily polluted, similar to the patterns of
699 Beijing, which may suggest the enhanced contribution of local traffic emissions in these two cities
700 during heavily polluted days. The chemical evolution of $\text{PM}_{2.5}$ at the background site of PRD was
701 similar to that of the urban site at Guangzhou, although a significant contribution of SIA was
702 observed when the pollution level increased from clean to moderately polluted (34% vs. 58%). Note
703 that the contribution of sulfate increased sharply, suggesting that regional transports dominated the
704 particle pollution during heavily polluted days. Compared with Beijing, a reversed chemical
705 evolution of $\text{PM}_{2.5}$ for the different pollution levels was observed in Shenyang, with the OM fraction
706 increasing sharply from 22% to 37%, while the SIA decreased slightly from 39% to 31% (Fig. 8c).
707 Note that a steady increase of sulfate from slightly polluted days to heavily polluted days was
708 observed. These results suggest that enhanced local emissions dominate the temporal evolution of
709 $\text{PM}_{2.5}$ on polluted days in Shenyang. A similar chemical evolution of $\text{PM}_{2.5}$ was found at the
710 background site of Changbai Mountain, which showed a significantly increased OM fraction and
711 slightly decrease of SIA when the pollution level increased from clean to slightly polluted,
712 indicating the enhanced contribution from local emissions like coal combustion for heating during
713 slightly polluted days. Further support for this pattern is seen in the increase of the EC fraction (Fig.
714 8 g). Similar to that in Guangzhou, the contribution of OM was almost constant for different



715 pollution levels in Chongqing. In addition, a much higher contribution of SIA was observed,
716 especially during the heavily polluted days, which suggests the importance of the formation of SIA
717 in driving PM_{2.5} pollution in Chongqing. The background site of Gongga Mountain shows decreased
718 contributions of OM, EC, SIA and mineral dust when the pollution level increased from clean to
719 slightly polluted days, similar to the pattern observed in Xinglong. Note that the unaccounted-for
720 fraction was largely increased on slightly polluted days (33% vs. 10%), possibly due to the increase
721 of aerosol-bound water related to the hygroscopic growth of aerosols at high RH values on slightly
722 polluted days (Bian et al., 2014). These results suggest the different formation mechanisms of the
723 heavy pollution in the most polluted city clusters, and unique mitigation measures should be
724 developed for the different regions of China.

725

726 4. Conclusions

727 We have established a national-level network (“Campaign on atmospheric Aerosol REsearch”
728 network of China (CARE-China)) that conducted continuous monitoring of PM_{2.5} mass
729 concentrations at 40 ground observation station, including 20 urban sites, 12 background sites and
730 8 rural/suburban sites. The average aerosol chemical composition was inferred from the filter
731 samples from six paired urban and background sites, which represent the largest megacities and
732 regional background areas in the five most polluted regions and the TAR of China. This study
733 presents the first long-term dataset including three-year observations of online PM_{2.5} mass
734 concentrations (2012-2014) and one year observations of PM_{2.5} compositions (2012-2013) from the
735 CARE-China network. One of the major purposes of this study was to compare and contrast urban
736 and background aerosol concentrations from nearby regions. The major findings include the
737 following:

738 (1) The average PM_{2.5} concentration from 20 urban sites is 73.2 µg/m³ (16.8-126.9 µg/m³), which
739 is three times greater than the average value of 12 background sites (11.2-46.5 µg/m³). The highest
740 PM_{2.5} concentrations were observed at the stations on the Guanzhong Plain (GZP) and the NCP. The
741 PM_{2.5} pollution is also a serious problem for the industrial regions of northeastern China and the
742 Sichuan Basin and is a relatively less serious problem for the YRD and the PRD. The background
743 PM_{2.5} concentrations of the NCP, YRD and PRD were comparable to those of the nearby urban sites,
744 especially for the PRD. A distinct seasonal variability of the PM_{2.5} is observed, presenting peaks
745 during the winter and minima during the summer at the urban sites, while the seasonal variations of
746 PM_{2.5} at the background sites vary in different part of China. Bimodal and unimodal diurnal
747 variation patterns were identified at both the urban and background stations.

748 (2) The major PM_{2.5} constituents across all the urban sites are OM (26.0%), SO₄²⁻ (17.7%),
749 mineral dust (11.8%), NO₃⁻ (9.8%), NH₄⁺ (6.6%), EC (6.0%), Cl⁻ (1.2%) at 45% RH and residual
750 matter (20.7%). Similar chemical compositions of PM_{2.5} were observed for the background sites
751 and were associated with higher fractions of OM (33.2%) and lower fractions of NO₃⁻ (8.6%) and
752 EC (4.1%). Analysis of filter samples reveals that several PM_{2.5} chemical components varied by
753 more than an order of magnitude between sites. For urban sites, the OM ranges from 12.6 µg/m³
754 (Lhasa) to 23.3 µg/m³ (Shenyang), the SO₄²⁻ ranges from 0.8 µg/m³ (Lhasa) to 19.7 µg/m³
755 (Chongqing), the NO₃⁻ ranges from 0.5 µg/m³ (Lhasa) to 11.9 µg/m³ (Shanghai) and the EC ranges
756 from 1.4 µg/m³ (Lhasa) to 7.1 µg/m³ (Guangzhou). The PM_{2.5} chemical species of the background



757 sites exhibit larger spatial heterogeneities than those of the urban sites, suggesting the different
758 contributions from regional anthropogenic and natural emissions and from the long-range transport
759 to background areas.

760 (3) Notable seasonal variations of $PM_{2.5}$ polluted days were observed, especially for the
761 megacities in east-central China, resulting in frequent heavy pollution episodes occurring during the
762 winter. The evolution of the chemical compositions of the $PM_{2.5}$ on polluted days was similar for
763 the urban and nearby background sites, suggesting the significant regional pollution characteristics
764 of the most polluted areas of China. However, the chemical species dominating the evolutions of
765 heavily polluted events were different in these areas. While sharply increasing contributions of SIA
766 and decreasing or constant contributions of OM during heavily polluted days were observed in
767 Beijing, Guangzhou and Chongqing, the reverse contributions of secondary inorganic aerosol and
768 OM were observed during the heavily polluted days of Shenyang. These results suggest that unique
769 mitigation measures should be developed for different regions of China.

770 The seasonal and spatial patterns of urban and background aerosols emphasize the importance
771 of understanding the variabilities of the concentrations of major aerosol species and their
772 contributions to the $PM_{2.5}$ budget. Comparisons of $PM_{2.5}$ chemical compositions from urban and
773 background sites of adjacent regions provided meaningful insights into aerosol sources and transport
774 and into the role of urban influences on nearby rural regions. The integration of data from 40 sites
775 from the CARE-China network provided an extensive spatial coverage of fine particle
776 concentrations near the surface and could be used to validate model results and implement effective
777 air pollution control strategies.

778

779 Acknowledgments

780 This study was supported by the Ministry of Science and Technology of China (Grant nos.
781 2017YFC0210000), the National Natural Science Foundation of China (Grant nos. 41705110) and
782 the Strategic Priority Research Program of the Chinese Academy of Sciences (Grant nos.
783 XDB05020200 & XDA05100100). We acknowledge the tremendous efforts of all the scientists and
784 technicians involved in the many aspects of the Campaign on atmospheric Aerosol REsearch
785 network of China (CARE-China).

786

787 References

- 788 Bell, M. L., Dominici, F., Ebisu, K., Zeger, S. L., and Samet, J. M.: Spatial and temporal variation in $PM_{2.5}$ chemical
789 composition in the United States for health effects studies. *Environ Health Perspect.*, 115, 989-995, 2007.
- 790 Bian, Y. X., Zhao, C. S., Ma, N., Chen, J., and Xu, W. Y.: A study of aerosol liquid water content based on
791 hygroscopicity measurements at high relative humidity in the North China Plain. *Atmos. Chem. Phys.*, 14, 6417-
792 6426, 2014.
- 793 Boyouk, N., León, J. F., Delbarre, H., Podvin, T., and Deroo, C.: Impact of the mixing boundary layer on the
794 relationship between $PM_{2.5}$ and aerosol optical thickness. *Atmos. Environ.*, 44(2), 271-277, 2010.
- 795 Chan, C. K., and Yao X. H.: Air pollution in mega cities in China. *Atmos. Environ.*, 42(1), 1-42, 2008.
- 796 Chen, W. H., Wang, X. M., Zhou, S. Z., Cohen, J. B., Zhang, J., Wang, Y., Chang, M., Zeng, Y., Liu, Y., Ling, Z.,
797 Liang, G., and Qiu, X.: Chemical Composition of $PM_{2.5}$ and its Impact on Visibility in Guangzhou, Southern China.
798 *Aerosol Air Qual. Res.*, 16, 2349-2361, 2016.



- 799 Chen, Y., Xie, S. D., Luo, B., and Zhai, C. Z.: Particulate pollution in urban Chongqing of southwest China:
800 Historical trends of variation, chemical characteristics and source apportionment. *Sci. Total Environ.*, 584-585, 523-
801 534, 2017.
- 802 Chen, Z., Wang, J. N., Ma, G. X., and Zhang, Y. S.: China tackles the health effects of air pollution. *Lancet*, 382,
803 1959-1960, 2013.
- 804 Cheng, Z., Wang, S., Fu, X., Watson, J. G., Jiang, J., Fu, Q., Chen, C., Xu, B., Yu, J., Chow, J. C., and Hao, J.: Impact
805 of biomass burning on haze pollution in the Yangtze River delta, China: a case study in summer 2011. *Atmos. Chem.*
806 *Phys.*, 14 (9), 4573-4585, 2014.
- 807 Cheng, Z., Luo, L., Wang, S., Wang, Y., Sharma, S., Shimadera, H., Wang, X., Bressi, M., Maura de Miranda, R.,
808 Jiang, J., Zhou, W., Fajardo, O., Yan, N., Hao, J.: Status and characteristics of ambient PM_{2.5} pollution in global
809 megacities. *Environ. Int.*, 89-90, 212-221, 2016.
- 810 Cong, Z., Kang, S., Luo, C., Li, Q., Huang, J., Gao, S. P., and Li, X. D.: Trace elements and lead isotopic composition
811 of PM₁₀ in Lhasa, Tibet. *Atmos. Environ.*, 45, 6210-6215, 2011.
- 812 Dickerson, R.R., Li, C., Li, Z., Marufu, L.T., Stehr, J.W., McClure, B., Krotkov, N., Chen, H., Wang, P., Xia, X.,
813 Ban, X., Gong, F., Yuan, J., and Yang, J.: Aircraft observations of dust and pollutants over northeast China: insight
814 into the meteorological mechanisms of transport. *J. Geophys. Res.*, 112, D24S90, doi: 10.1029/2007JD008999, 2007.
- 815 Eeftens, M., Tsai, M.-Y., Ampe, C., Anwander, B., Beelen, R., Bellander, T., Cesaroni, G., Cirach, M., Cyrys, J.,
816 Hoogh, K. D., Nazelle, A. D., Vocht, F. D., Declercq, C., Dedele, A., Eriksen, K., Galassi, C., Grazuleviciene, R.,
817 Grivas, G., Heinrich, J., Hoffmann, B., Iakovides, M., Ineichen, A., Katsouyanni, K., Korek, M., Krämer, U.,
818 Kuhlbusch, T., Lanki, T., Madsen, C., Meliefste, K., Mölter, A., Mosler, G., Nieuwenhuijsen, M., Oldenwening,
819 M., Pennanen, A., Probst-Hensch, N., Quass, U., Raaschou-Nielsen, O., Ranzi, A., Stephanou, E., Sugiri, D.,
820 Udvardy, O., Vaskövi, É., Weinmayr, G., Brunekreef, B., and Hoek, G.: Spatial variation of PM_{2.5}, PM₁₀, PM_{2.5}
821 absorbance and PM coarse concentrations between and within 20 European study areas and the relationship with
822 NO₂ - Results of the ESCAPE project. *Atmos. Environ.*, 62, 303-317, 2012.
- 823 Fu, X., Wang, S. X., Zhao, B., Xing, J., Cheng, Z., Liu, H., and Hao, J. M.: Emission inventory of primary pollutants
824 and chemical speciation in 2010 for the Yangtze River Delta region, China. *Atmos. Environ.*, 70, 39-50, 2013.
- 825 Fu, X., Wang, S. X., Cheng, Z., Xing, J., Zhao, B., Wang, J. D., and Hao, J. M.: Source, transport and impacts of a
826 heavy dust event in the Yangtze River Delta, China, in 2011. *Atmos. Chem. Phys.*, 14 (3), 1239-1254, 2014.
- 827 Gehrig, R., and Buchmann, B.: Characterising seasonal variations and spatial distribution of ambient PM₁₀ and PM_{2.5}
828 concentrations based on long-term Swiss monitoring data. *Atmos. Environ.*, 37, 2571-2580, 2003.
- 829 Guo, S., Hu, M., Zamora, M. L., Peng, J., Shang, D., Zheng, J., Du, Z., Wu, Z., Shao, M., Zeng, L., Molina, M. J.,
830 and Zhang, R.: Elucidating severe urban haze formation in China. *Proc. Nat. Acad. Sci. U.S.A.* 111, 17373-17378,
831 2014.
- 832 Hand, J. L., Schichtel, B. A., Pitchford, M., Malm, W. C., and Frank, N. H.: Seasonal composition of remote and
833 urban fine particulate matter in the United States. *J. Geophys. Res.*, 117, D05209, doi: 10.1029/2011JD017122, 2012.
- 834 He, K. B., Yang, F. M., Ma, Y. L., Zhang, Q., Yao, X. H., Chan, C. K., Cadle, S., Chan, T., and Mulawa, P.: The
835 characteristics of PM_{2.5} in Beijing, China. *Atmos. Environ.*, 35(29), 4959-4970, 2001.
- 836 Hoffer, A., Gelencser, A., Guyon, P., Kiss, G., Schmid, O., Frank, G. P., Artaxo, P. and Andreae, M. O.: Optical
837 properties of humic-like substances (HULIS) in biomass-burning aerosols. *Atmos. Chem. Phys.*, 6, 3563-3570, 2006.
- 838 Huang, R. J., Zhang, Y., Bozzetti, C., Ho, K., Cao, J., Han, Y., Daellenbach, K., Slowik, J., Platt, S., Canonaco, F.,
839 Zotter, P., Wolf, R., Pieber, S., Bruns, E., Crippa, M., Ciarelli, G., Piazzalunga, A., Schwikowski, M., Abbaszade,
840 G., Schnelle-Kreis, J., Zimmermann, R., An, Z., Szidat, S., Baltensperger, U., Haddad, I., and Prévôt, A.: High



- 841 secondary aerosol contribution to particulate pollution during haze events in China. *Nature*, 514, 218-222, 2014.
- 842 Huang, Y., Li, L., Li, J., Wang, X., Chen, H., Chen, J., Yang, X., Gross, D. S., Wang, H., Qiao, L., and Chen, C.: A
- 843 case study of the highly time-resolved evolution of aerosol chemical and optical properties in urban Shanghai, China.
- 844 *Atmos. Chem. Phys.*, 13(8), 3931-3944, 2013.
- 845 IPCC: Climate Change 2013: The Physical Science Basis: Summary for Policymakers, Cambridge, UK, 2013.
- 846 Janssen, N. A. H., Fischer, P., Marra, M., Ameling, C., and Cassee, F. R.: Short-term effects of PM_{2.5}, PM₁₀ and
- 847 PM_{2.5-10} on daily mortality in the Netherlands. *Sci. Total Environ.*, 463-464, 20-26, 2013.
- 848 Li, L., Chen, C. H., Fu, J. S., Huang, C., Streets, D. G., Huang, H. Y., Zhang, G. F., Wang, Y. J., Jang, C. J., Wang,
- 849 H. L., Chen, Y. R., and Fu, J. M.: Air quality and emissions in the Yangtze River Delta, China. *Atmos. Chem. Phys.*,
- 850 11, 1621-1639, 2011
- 851 Li, Y. C., Yu, J. Z., Ho, S. S. H., Yuan, Z. B., Lau, A. K. H., and Huang X. F.: Chemical characteristics of PM_{2.5} and
- 852 organic aerosol source analysis during cold front episodes in Hong Kong, China. *Atmos. Res.*, 118, 41-51, 2012.
- 853 Liu, Z. R., Hu, B., Wang, L. L., Wu, F. K., Gao, W. K., and Wang, Y. S.: Seasonal and diurnal variation in particulate
- 854 matter (PM₁₀ and PM_{2.5}) at an urban site of Beijing: analyses from a 9-year study. *Environ. Sci. Pollut. Res.*, 22, 627-
- 855 642, 2015.
- 856 Liu, L., Zhang, X., Wang, S., Zhang, W., and Lu, X.: Bulk sulfur (S) deposition in China. *Atmos. Environ.*, 135, 41-
- 857 49, 2016b.
- 858 Liu, Z. R., Wang, Y. S., Hu, B., Ji, D. S., Zhang, J. K., Wu, F. K., Wan, X. and Wang, Y. H.: Source appointment of
- 859 fine particle number and volume concentration during severe haze pollution in Beijing in January 2013. *Environ.*
- 860 *Sci. Pollut. Res.*, 23(7), 6845-6860, 2016a.
- 861 Liu, Z. R., Wang, Y. S., Liu, Q., Liu, L. N., and Zhang, D. Q.: Pollution Characteristics and Source of the Atmospheric
- 862 Fine Particles and Secondary Inorganic Compounds at Mount Dinghu in Autumn Season (in Chinese). *Environ. Sci.*,
- 863 32, 3160-3166, 2011.
- 864 Lu, Z., Streets, D. G., Zhang, Q., Wang, S., Carmichael, G. R., Cheng, Y. F., Wei, C., Chin, M., Dieh, T., and Tan,
- 865 Q.: Sulfur dioxide emissions in China and sulfur trends in East Asia since 2000. *Atmos. Chem. Phys.*, 10, 6311-6331,
- 866 2010.
- 867 Malm, W. C., Schichtel, B. A., Pitchford, M. L., Ashbaugh, L. L., and Eldred, R. A.: Spatial and monthly trends in
- 868 speciated fine particle concentration in the United States. *J. Geophys. Res.*, 109, D03306, doi:
- 869 10.1029/2003JD003739, 2004.
- 870 Mamtimin, B., and Meixner, F. X.: Air pollution and meteorological processes in the growing dryland city of Urumqi
- 871 (Xinjiang, China). *Sci. Total Environ.*, 409(7), 1277-1290, 2011.
- 872 Mao, Y. H., Liao, H., and Chen, H. S.: Impacts of East Asian summer and winter monsoons on interannual variations
- 873 of mass concentrations and direct radiative forcing of black carbon over eastern China. *Atmos. Chem. Phys.*, 17,
- 874 4799-4816, 2017.
- 875 Mauderly, J. L., and Chow, J. C.: Health effects of organic aerosols. *Inhal. Toxicol.*, 20, 257-288, 2008.
- 876 Niu, Z. C., Zhang, F. W., Chen, J. S., Yin, L. Q., Wang, S., and Xu, L. L.: Carbonaceous species in PM_{2.5} in the
- 877 coastal urban agglomeration in the Western Taiwan Strait Region, China. *Atmos. Res.*, 122, 102-110, 2013.
- 878 Oanh, N. T. K., Upadhyay, N., Zhuang, Y. H., Hao, Z. P., Murthy, D. V. S., Lestari, P., Villarin, J. T., Chengchua, K.,
- 879 Co, H. X., Dung, N. T., and Lindgren, E. S.: Particulate air pollution in six Asian cities: Spatial and temporal
- 880 distributions, and associated sources. *Atmos. Environ.*, 40, 3367-3380, 2006.
- 881 Pan, Y. P., Wang, Y. S., Sun, Y., Tian, S. L., and Cheng, M. T.: Size-resolved aerosol trace elements at a rural
- 882 mountainous site in Northern China: Importance of regional transport. *Sci. Total Environ.*, 461, 761-771, 2013.



- 883 Patashnick, H., and Rupprecht, E.: Continuous PM₁₀ measurements using the tapered element oscillating
884 microbalance. *J. Air Waste Manage.*, 41, 1079-1083, 1991.
- 885 Putaud, J. P., Van Dingenen, R., Alastuey, A., Bauer, H., Birmili, W., Cyrys, J., Flentje, H., Fuzzi, S., Gehrig, R.,
886 Hansson, H. C., Harrison, R. M., Herrmann, H., Hitznerberger, R., Hüglin, C., Jones, A. M., Kasper-Giebl, A., Kiss,
887 G., Kousa, A., Kuhlbusch, T. A. J., Löschau, G., Maenhaut, W., Molnar, A., Moreno, T., Pekkanen, J., Perrino, C.,
888 Pitz, M., Puxbaum, H., Querol, X., Rodriguez, S., Salma, I., Schwarz, J., Smolik, J., Schneider, J., Spindler, G., ten
889 Brink, H., Tursic, J., Viana, M., Wiedensohler, A., and Raes, F.: A European aerosol phenomenology - 3: Physical
890 and chemical characteristics of particulate matter from 60 rural, urban, and kerbside sites across Europe. *Atmos.*
891 *Environ.*, 44, 1308-1320, 2010.
- 892 Quan, J. N., Tie, X. X., Zhang, Q., Liu, Q., Li, X., Gao, Y., and Zhao, D. L.: Characteristics of heavy aerosol pollution
893 during the 2012-2013 winter in Beijing, China. *Atmos. Environ.*, 88, 83-89, 2014.
- 894 Seinfeld, J. H., and Pandis, S. N.: *Atmospheric Chemistry and Physics: from Air Pollution to Climate Change*. Wiley,
895 New York, USA, 2016.
- 896 Sun, Q. H., Hong, X. R., and Wold, L. E.: Cardiovascular Effects of Ambient Particulate Air Pollution Exposure.
897 *Circulation*, 121(25), 2755-2765, 2010.
- 898 Tao, J., Zhang, L. M., Ho, K. F., Zhang, R. J., Lin, Z. J., Zhang, Z. S., Lin, M., Cao, J. J., Liu, S. X., and Wang, G.
899 H.: Impact of PM_{2.5} chemical compositions on aerosol light scattering in Guangzhou - the largest megacity in South
900 China. *Atmos. Res.*, 135, 48-58, 2014.
- 901 Tao, J., Zhang, L. M., Cao, J. J., Zhong, L. J., Chen, D. S., Yang, Y. H., Chen, D. H., Chen, L. G., Zhang, Z. S., Wu,
902 Y. F., Xia, Y. J., Ye, S. Q., and Zhang, R. J.: Source apportionment of PM_{2.5} at urban and suburban areas of the Pearl
903 River Delta region, south China - With emphasis on ship emissions. *Sci. Total Environ.*, 574, 1559-1570, 2017.
- 904 Turpin, B. J., and Lim, H. J.: Species contributions to PM_{2.5} mass concentrations: Revisiting common assumptions
905 for estimating organic mass. *Aerosol Sci. Technol.*, 35, 602-610, 2001.
- 906 Verma, R. L., Sahu, L. K., Kondo, Y., Takegawa, N., Han, S., Jung, J. S., Kim, Y. J., Fan, S., Sugimoto, N., Shammaa,
907 M. H., Zhang, Y. H., and Zhao, Y.: Temporal variations of black carbon in Guangzhou, China, in summer 2006.
908 *Atmos. Chem. Phys.*, 10, 6471-6485, 2010.
- 909 Viana, M., X., Querol, A., Alastuey, F., Ballester, S., Llop, A., Esplugues, R., Fernandez-Patier, S., dos Santos, G.,
910 and Hecce, M. D.: Characterising exposure to PM aerosols for an epidemiological study. *Atmos. Environ.*, 42(7),
911 1552-1568, 2008.
- 912 Wan, X., Kang, S. C., Xin, J. Y., Liu, B., Wen, T. X., Wang, P. L., Wang, Y. S., and Cong, Z. Y.: Chemical composition
913 of size-segregated aerosols in Lhasa city, Tibetan Plateau. *Atmos. Res.*, 174-175, 142-150, 2016.
- 914 Wang, Y. S., Yao, L., Wang, L. L., Liu, Z. R., Ji, D. S., Tang, G. Q., Zhang, J. K., Sun, Y., Hu, B., and Xin, J. Y.:
915 Mechanism for the formation of the January 2013 heavy haze pollution episode over central and eastern China. *Sci.*
916 *China: Earth Sci.*, 57, 14-25, 2014.
- 917 Wang, G. H., Zhou, B. H., Cheng, C. L., Cao, J. J., Li, J. J., Meng, J. J., Tao, J., Zhang, R. J., and Fu, P. Q.: Impact
918 of Gobi desert dust on aerosol chemistry of Xi'an, inland China during spring 2009: differences in composition and
919 size distribution between the urban ground surface and the mountain atmosphere. *Atmos. Chem. Phys.*, 13(2), 819-
920 835, 2013.
- 921 Wang, H. L., Qiao, L. P., Lou, S. R., Zhou, M., Ding, A. J., Huang, H. Y., Chen, J. M., Wang, Q., Tao, S. K., Chen,
922 C. H., Li, L., and Huang, C.: Chemical composition of PM_{2.5} and meteorological impact among three years in urban
923 Shanghai, China. *J. Clean. Prod.*, 112, 1302-1311, 2016.
- 924 Wang, Y. Q., Zhang, X. Y., Sun, J. Y., Zhang, X. C., Che, H. Z., and Li, Y.: Spatial and temporal variations of the



- 925 concentrations of PM₁₀, PM_{2.5} and PM₁ in China. *Atmos. Chem. Phys.*, 15, 13585-13598, 2015.
- 926 Wu, F. K., Yu, Y., Sun, J., Zhang, J. K., Wang, J., Tang, G. Q., and Wang, Y. S.: Characteristics, source apportionment
927 and reactivity of ambient volatile organic compounds at Dinghu Mountain in Guangdong Province, China. *Sci. Total*
928 *Environ.*, 548-549, 347-359, 2016.
- 929 Xia, X. A., Chen, H. B., Wang, P. C., Zhang, W. X., Goloub, P., Chatenet, B., Eck, T. F., and Holben, B. N.: Variation
930 of column-integrated aerosol properties in a Chinese urban region. *J. Geophys. Res.-Atmos.*, 111, D05204, doi:
931 10.1029/2005JD006203, 2006.
- 932 Xin, J., Wang, Y., Wang, L., Tang, G., Sun, Y., Pan, Y., and Ji, D.: Reductions of PM_{2.5} in Beijing-Tianjin-Hebei
933 urban agglomerations during the 2008 Olympic Games. *Adv. Atmos. Sci.*, 29(6), 1330-1342, 2012.
- 934 Xing, L., Fu, T. M., Cao, J. J., Lee, S. C., Wang, G. H., Ho, K. F., Cheng, M. C., You, C. F., and Wang, T. J.: Seasonal
935 and spatial variability of the OM/OC mass ratios and high regional correlation between oxalic acid and zinc in
936 Chinese urban organic aerosols. *Atmos. Chem. Phys.*, 13, 4307-4318, 2013.
- 937 Xu, J. S., Xu, M. X., Snape, C., He, J., Behera, S. N., Xu, H. H., Ji, D. S., Wang, C. J., Yu, H., Xiao, H., Jiang, Y. J.,
938 Qi, B., and Du, R. G.: Temporal and spatial variation in major ion chemistry and source identification of secondary
939 inorganic aerosols in Northern Zhejiang Province, China. *Chemosphere*, 179, 316-330, 2017.
- 940 Yang, F., Tan, J., Zhao, Q., Du, Z., He, K., Ma, Y., Duan, F., and Chen, G.: Characteristics of PM_{2.5} speciation in
941 representative megacities and across China. *Atmos. Chem. Phys.*, 11(11), 5207-5219, 2011.
- 942 Ye, B., Ji, X., Yang, H., Yao, X., Chan, C. K., Cadle, S. H., Chan, T., and Mulawa, P. A.: Concentration and chemical
943 composition of PM_{2.5} in Shanghai for a 1-year period. *Atmos. Environ.*, 37, 499-510, 2003.
- 944 Zhang, C., Zhou, R., and Yang, S.: Implementation of clean coal technology for energy-saving and emission
945 reduction in Chongqing. *Environment and Ecology in the Three Gorges (in Chinese)*, 3, 52-56, 2010.
- 946 Zhang, J. K., Sun, Y., Wu, F. K., Sun, J., and Wang, Y. S.: The characteristics, seasonal variation and source
947 apportionment of VOCs at Gongga Mountain, China. *Atmos. Environ.*, 88, 297-305, 2014c.
- 948 Zhang, L. W., Chen, X., Xue, X. D., Sun, M., Han, B., Li, C. P., Ma, J., Yu, H., Sun, Z. R., Zhao, L. J., Zhao, B. X.,
949 Liu, Y. M., Chen, J., Wang, P. P., Bai, Z. P., and Tang, N. J.: Long-term exposure to high particulate matter pollution
950 and cardiovascular mortality: A 12-year cohort study in four cities in northern China. *Environ. Int.*, 62, 41-47, 2014a.
- 951 Zhang, N. N., Cao, J. J., Liu, S. X., Zhao, Z. Z., Xu, H. M., and Xiao, S.: Chemical composition and sources of PM_{2.5}
952 and TSP collected at Qinghai Lake during summertime. *Atmos. Res.*, 138, 213-222, 2014b.
- 953 Zhang, X. Y., Wang, Y. Q., Niu, T., Zhang, X. C., Gong, S. L., Zhang, Y. M., and Sun, J. Y.: Atmospheric aerosol
954 compositions in China: spatial/temporal variability, chemical signature, regional haze distribution and comparisons
955 with global aerosols. *Atmos. Chem. Phys.* 12 (2), 779-799, 2012.
- 956 Zhang, Y. L., and Cao, F.: Fine particulate matter (PM_{2.5}) in China at a city level. *Sci. Rep.*, 5: 14884, 2015.
- 957 Zhao, M. F., Huang, Z. S., Qiao, T., Zhang, Y. K., Xiu, G. L., and Yu, J. Z.: Chemical characterization, the transport
958 pathways and potential sources of PM_{2.5} in Shanghai: seasonal variations. *Atmos. Res.*, 158, 66-78, 2015.
- 959 Zhao, P. S., Dong, F., Yang, Y. D., He, D., Zhao, X. J., Zhang, W. Z., Yao, Q., and Liu, H. Y.: Characteristics of
960 carbonaceous aerosol in the region of Beijing, Tianjin, and Hebei, China. *Atmos. Environ.*, 71, 389-398, 2013a.
- 961 Zhao, X. J., Zhao, P. S., Xu, J., Meng, W., Pu, W. W., Dong, F., He, D., and Shi, Q. F.: Analysis of a winter regional
962 haze event and its formation mechanism in the North China Plain. *Atmos. Chem. Phys.*, 13(11), 5685-5696, 2013b.
- 963 Zheng, J., Zhang, L., Che, W., Zheng, Z., and Yin, S.: A highly resolved temporal and spatial air pollutant emission
964 inventory for the Pearl River Delta region, China and its uncertainty assessment. *Atmos. Environ.* 43, 5112-5122,
965 2009.
- 966 Zhou, S. Z., Wang, Z., Gao, R., Xue, L., Yuan, C., Wang, T., Gao, X., Wang, X., Nie, W., Xu, Z., Zhang, Q., and



- 967 Wang, W.: Formation of secondary organic carbon and long-range transport of carbonaceous aerosols at Mount Heng
968 in South China. *Atmos. Environ.*, 63, 203-212, 2012.
- 969 Zimmermann, R.: Aerosols and health: a challenge for chemical and biological analysis. *Anal Bioanal Chem.*, 407,
970 5863-5867, 2015.
- 971 Zou, X. K., and Zhai, P. M.: Relationship between vegetation coverage and spring dust storms over northern China.
972 *J. Geophys. Res.*, 109, D03104, doi: 10.1029/2003JD003913, 2004.
- 973

974 Table 1 Geographic information and three-year mean PM_{2.5} concentration of the monitor stations.

Station/Code	Latitude, Longitude	Altitude(m)	Station type	Mean($\mu\text{g}/\text{m}^3$)	N(day)
Beijing/BJC	39.97 N, 116.37 E	45	Northern city	69.4 \pm 54.8	1077
Cele/CLD	37.00 N, 80.72 E	1306	Northwestern country	126.9 \pm 155.4	600
Changbai Mountain/CBM	42.40 N, 128.01 E	738	Northeastern background	17.6 \pm 12.6	807
Changsha/CSC	28.21 N, 113.06 E	45	Central city	77.9 \pm 45.4	1045
Chengdu/CDC	30.67 N, 104.06 E	506	Southwestern city	102.2 \pm 66.2	1008
Chongqing/CQC	29.59 N, 106.54 E	259	Southwestern city	65.1 \pm 35.8	972
Dinghu Mountain/DHM	23.17 N, 112.50 E	90	Pearl River Delta background	40.1 \pm 25.0	954
Dunhuang/DHD	40.13 N, 94.71 E	1139	Desert town	86.2 \pm 94.3	726
Fukang/FKZ	44.28 N, 87.92 E	460	Northwestern country	69.9 \pm 69.6	960
Gongga Mountain/GGM	29.51 N, 101.98 E	1640	Southwestern background	25.5 \pm 15.5	869
Guangzhou/GZC	23.16 N, 113.23 E	43	Southern city	44.1 \pm 23.8	772
Hailun/HLA	47.43 N, 126.63 E	236	Northeastern country	41.6 \pm 45.0	1076
Hefei/HFC	31.86 N, 117.27 E	24	Eastern city	80.4 \pm 45.3	909
Ji'nan/JNC	36.65 N, 117.00 E	70	Northern city	107.8 \pm 57.4	701
Kunming/KMC	25.04 N, 102.73 E	1895	Southwestern city	47.0 \pm 25.2	967
Lhasa/LSZ	29.67 N, 91.33 E	3700	Tibet city	30.6 \pm 21.3	600
Lin'an/LAZ	30.30 N, 119.73 E	139	Eastern background	46.5 \pm 27.2	1086
Mount Everest/ZFM	28.21 N, 86.56 E	4700	Tibet background	24.4 \pm 25.1	390
Namtso/NMT	30.77 N, 90.98 E	4700	Tibet background	11.2 \pm 6.9	499
Nagri/ALZ	32.52 N, 79.89 E	4300	Tibet background	19.5 \pm 12.4	72
Qianyanzhou/QYZ	26.75 N, 115.07 E	76	Southeastern country	52.1 \pm 28.4	927
Qinghai Lake/QHL	37.62 N, 101.32 E	3280	Tibet background	16.2 \pm 17.0	590
Sanya/SYB	18.22 N, 109.47 E	8	Southern island city	16.8 \pm 13.1	595
Shanghai/SHC	31.22 N, 121.48 E	9	Eastern city	56.2 \pm 59.4	822
Shapotou/SPD	37.45 N, 104.95 E	1350	Desert background	51.1 \pm 33.3	1016
Shenyang/SYC	41.50 N, 123.40 E	49	Northeastern city	77.6 \pm 41.2	926
Shijiazhuang/SJZ	38.03 N, 114.53 E	70	Northern city	105.1 \pm 92.7	1031
Taipei/TBC	25.03 N, 121.90 E	150	Island city	22.1 \pm 10.7	1083
Taiyuan/TYC	37.87 N, 112.53 E	784	Northern city	111.5 \pm 74.9	987
Tianjin/TJC	39.08 N, 117.21 E	9	Northern city	69.9 \pm 49.6	1034
Tongyu/TYZ	44.42 N, 122.87 E	160	Inner Mongolia background	24.5 \pm 24.5	757
Urumchi/URC	43.77 N, 87.68 E	918	Northwestern city	104.1 \pm 145.2	776
Wuxi/WXC	31.50 N, 120.35 E	5	Eastern city	65.2 \pm 36.8	1003
Xi'An/XAC	34.27 N, 108.95 E	397	Central city	125.8 \pm 108.2	1077
Xianghe/XHZ	39.76 N, 116.95 E	25	North China suburbs	83.7 \pm 62.3	1084
Xinglong/XLZ	40.40 N, 117.58 E	900	North China background	39.8 \pm 34.0	1035
Xishuangbanna/BNF	21.90 N, 101.27 E	560	Southwestern rain forest	25.0 \pm 18.7	707
Yantai/YTZ	36.05 N, 120.27 E	47	East China sea coast city	51.1 \pm 36.7	915
Yucheng/YCA	36.95 N, 116.60 E	22	North China country	102.8 \pm 61.8	1008
Zangdongnan/ZDN	29.77 N, 94.73 E	2800	Southern Tibet forest	12.3 \pm 8.0	475

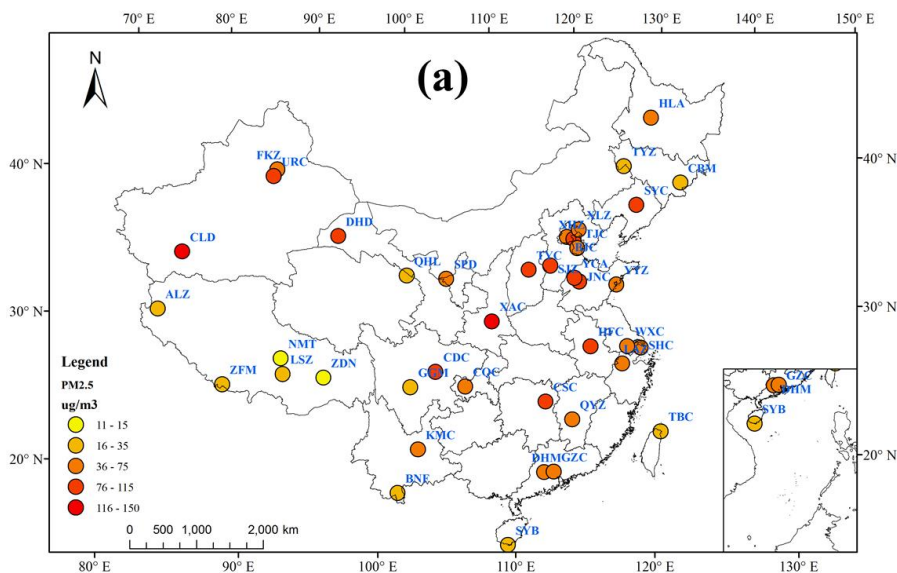


975 Table 2 Summary of the concentrations of PM_{2.5} and its components (µg/m³) in urban and
 976 background sites.

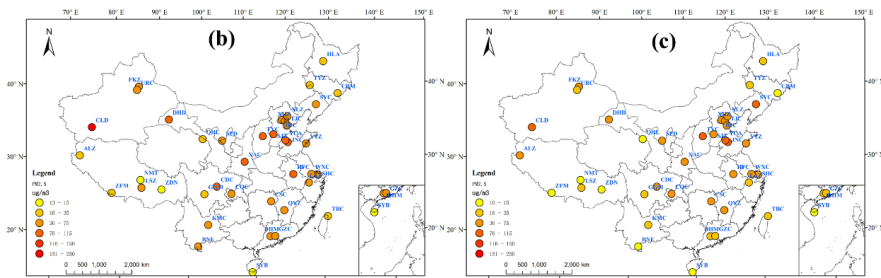
Station	PM _{2.5}	OM	EC	NO ₃ ⁻	SO ₄ ²⁻	NH ₄ ⁺	MD*	Cl ⁻	Unaccounted
Urban sites									
Beijing(n=88)	71.7	19.1	4.1	9.3	11.9	5.3	4.7	0.7	16.5
Shanghai(n=120)	68.4	17.1	2.0	11.9	13.6	5.8			18.1
Guangzhou(n=106)	75.3	16.7	7.1	7.2	13.1	4.8	7.3	1.0	18.1
Lhasa(n=60)	36.4	12.6	1.4	0.5	0.8	0.4	11.6	0.3	8.8
Shenyang(n=36)	81.8	23.3	5.2	4.6	13.2	4.5	9.2	1.4	20.4
Chongqing(n=56)	73.5	17.2	4.8	6.5	19.7	6.1	7.4	0.6	11.2
Background sites									
Xinglong(n=42)	42.6	12.4	1.5	3.7	8.4	3.4	5.0	0.3	7.9
Lin'an(n=60)	66.3	21.7	2.9	8.7	11.2	7.3	2.0	0.6	11.9
Dinghu Mountain(n=36)	40.1	11.6	2.0	4.5	10.1	4.0	3.8	0.5	3.6
Namsto(n=35)	9.5	3.4	0.2	0.1	0.4	0.4	3.9	0.1	1.1
Changbai Mountain(n=52)	23.3	8.9	0.9	1.1	3.3	1.8	3.7	0.2	3.5
Gongga Mountain(n=36)	32.2	13.1	1.1	0.4	4.7	1.7	3.2	0.4	7.7

977 *MD: mineral dust

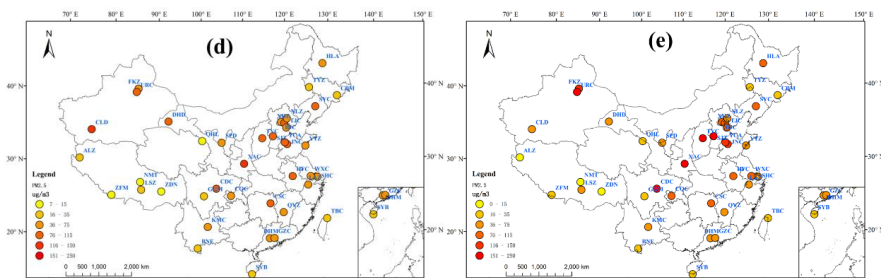
978



979



980



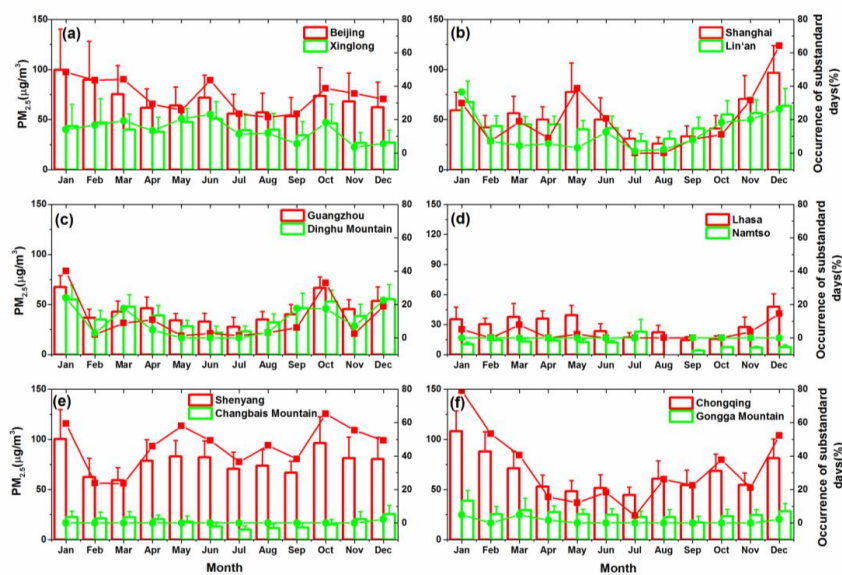
981

982 Fig.1. Locations and the averaged PM_{2.5} concentrations of the forty monitor stations during (a) the
 983 year of 2012-2014, (b) spring, (c) summer, (d) autumn and (e) winter

984

985

986



987

988

989

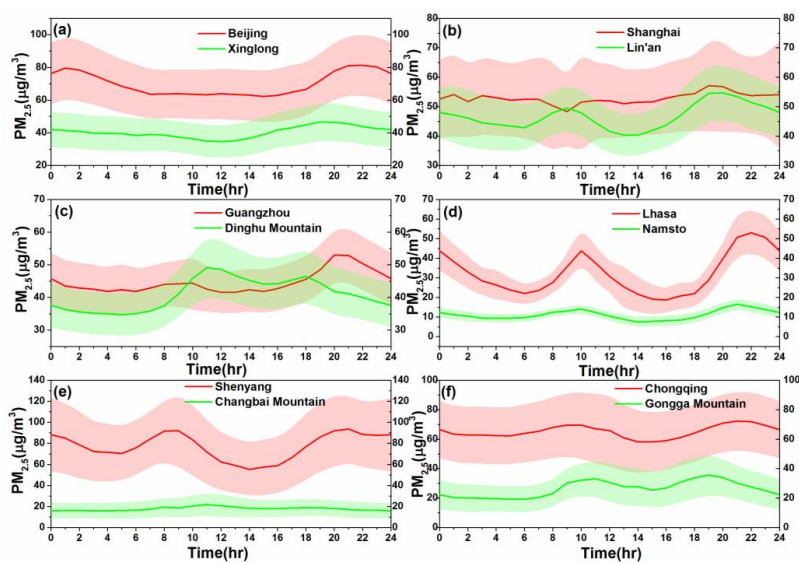
990

991

992

993

Fig.2. Monthly average $PM_{2.5}$ concentration (histogram, left coordinate) and the occurrence of substandard days in each month (dotted line, right coordinate) at urban and background sites in (a)North China plain, (b)Yangtze River delta, (c) Pearl River delta, (d)Tibetan Autonomous Region, (e) Northeast China Region and (f) Southwestern China Region. The error bar stands for the standard deviation.



994

995

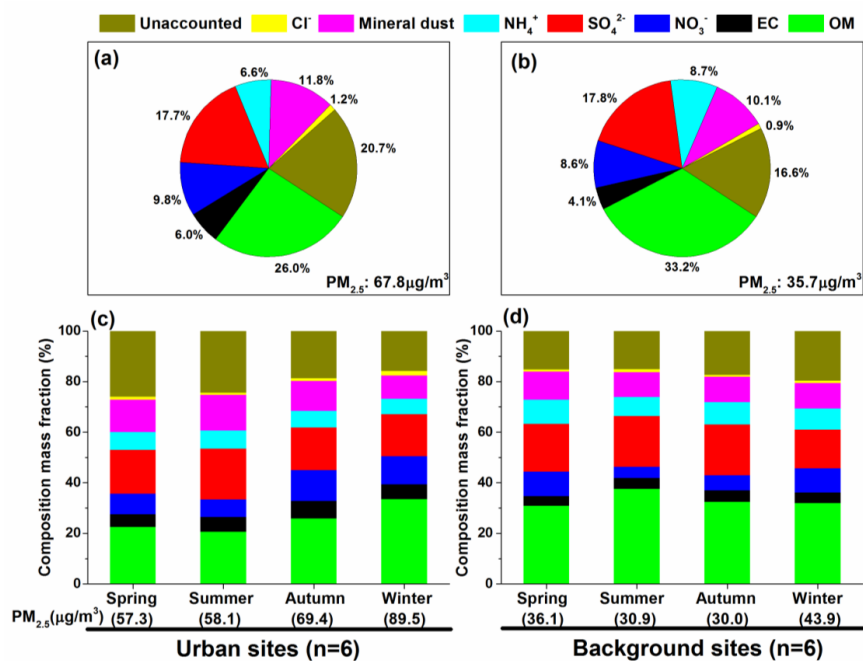
996 Fig.3 Diurnal cycles of $PM_{2.5}$ at six paired urban and background sites in (a)North China plain,

997

998

(b)Yangtze River delta, (c) Pearl River delta, (d)Tibetan Autonomous Region, (e) Northeast China

Region and (f) Southwestern China Region.

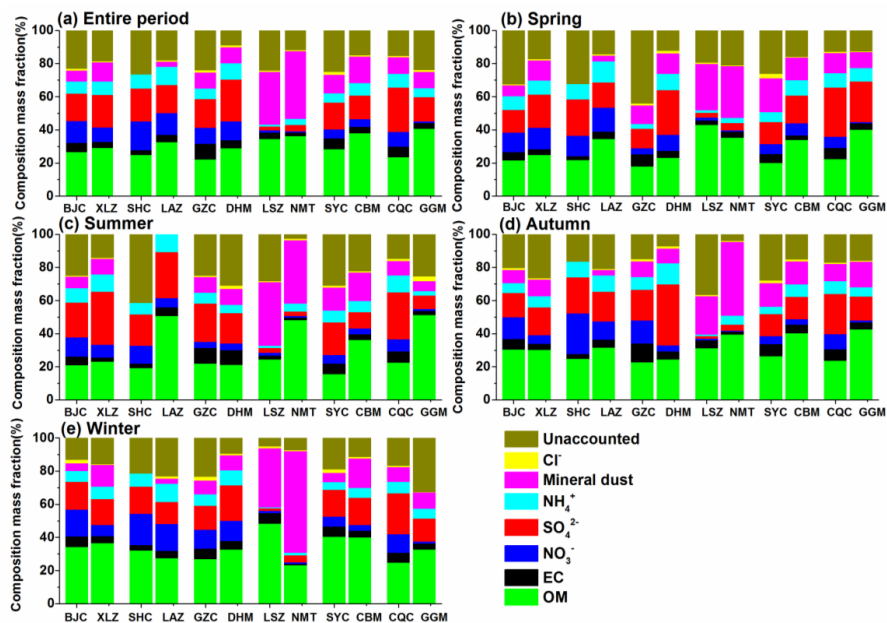


999
 1000
 1001
 1002
 1003

Fig.4 Average chemical composition and its seasonal variations of PM_{2.5} in (a, c) urban sites and (b, d) background sites.



1004

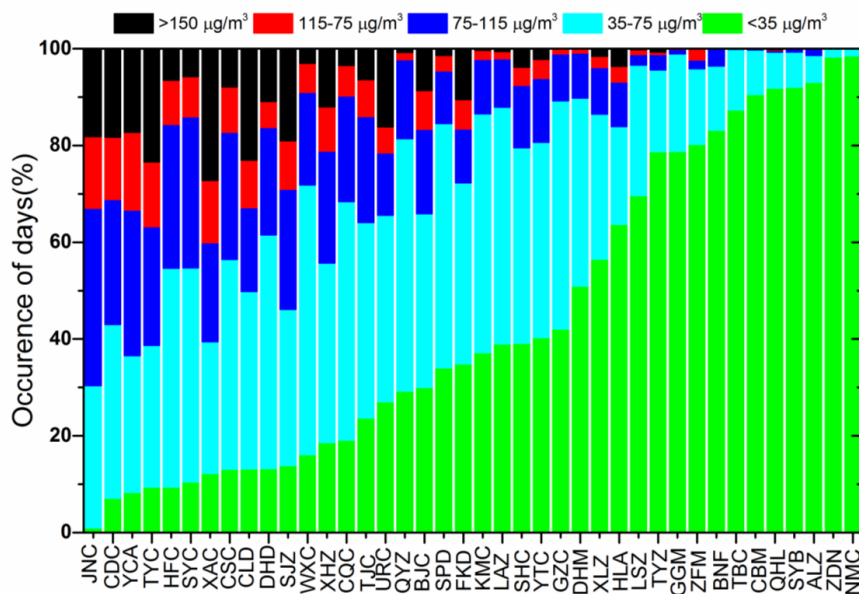


1005

1006

1007

Fig.5 Average chemical composition of PM_{2.5} in (a) urban sites and (b) background sites.



1008

1009

1010

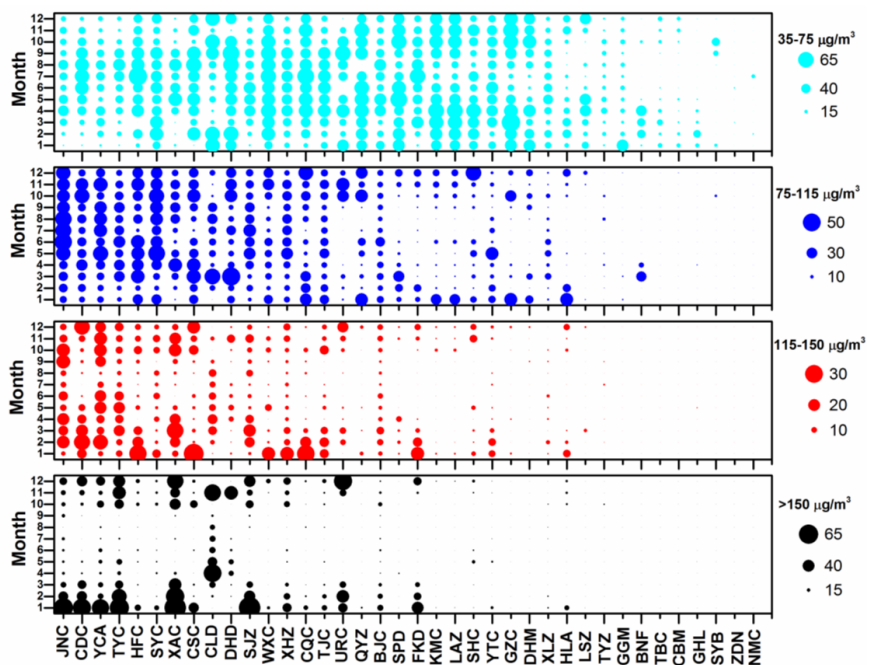
1011

1012

1013

1014

Fig.6 Days separated by the threshold values of the “Ambient Air Quality Standard” (AAQS) (GB3095-2012) of China guideline. The threshold values of 35, 75, 115 and 150µg/m³ used for the daily concentration ranges are represented as clean (<35µg/m³), slightly polluted (35-75µg/m³), moderated polluted (75-115µg/m³), polluted (115-150µg/m³) and heavily polluted (>150µg/m³), which suggested by the guideline of the AAQS.



1015

1016

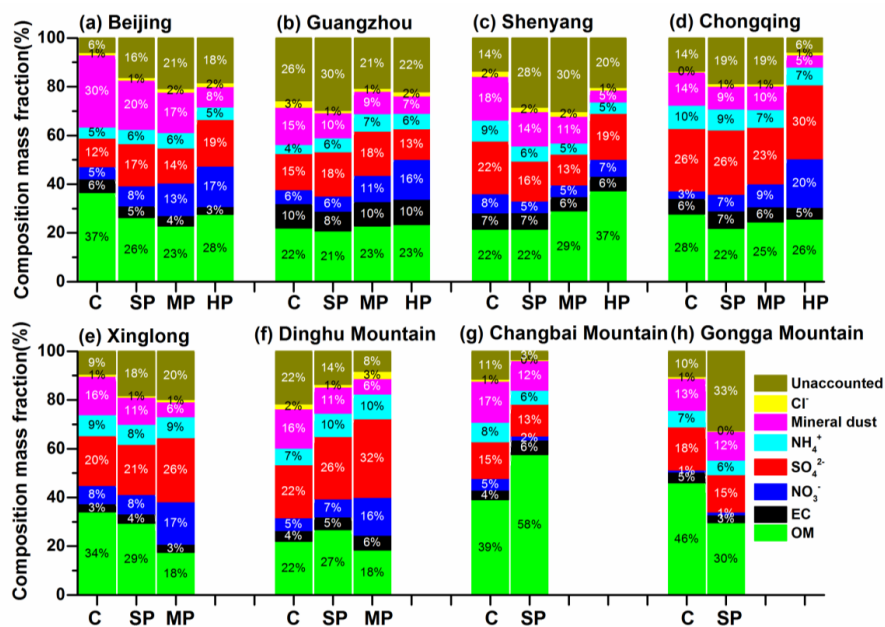
1017

1018

1019

1020

Fig.7 Monthly distribution of the occurrence of the polluted days exceeding the “Ambient Air Quality Standard” (AAQS) (GB3095-2012) of China. The symbol size represents the occurrences of polluted days for the corresponding month. The symbol color represents the different mass range. The sites of Nagri and Mount Everest are excluded because of the small sample size.



1021
 1022 Fig. 8 Average chemical composition of PM_{2.5} with respect to pollution level. The C, SP, MP and
 1023 HP is related to clean (daily PM_{2.5} < 35 μg/m³), slightly polluted (35 μg/m³ < daily PM_{2.5} < 75 μg/m³),
 1024 moderated polluted (75 μg/m³ < daily PM_{2.5} < 150 μg/m³) and heavily polluted (daily PM_{2.5} > 150
 1025 μg/m³).
 1026
 1027